HEAT TRANSFER DURING FILM CONDENSATION OF POTASSIUM VAPOR ON A HORIZONTAL PLATE

Paul M. Meyrial
Michel L. Morin
Warren M. Rohsenow

Report No. DSR 70008-52

Contract No. GK-1113

Department of Mechanical Engineering
Engineering Projects Laboratory
Massachusetts Institute of Technology

March 1, 1968

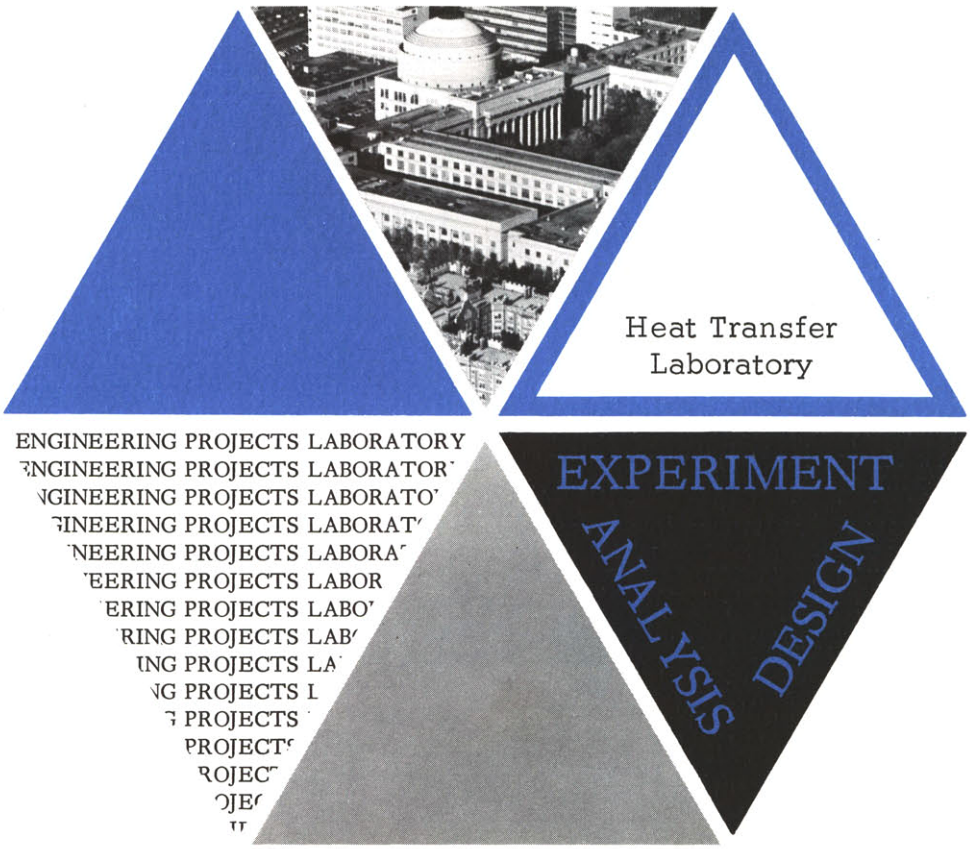

HEAT TRANSFER DURING FILM CONDENSATION OF POTASSIUM VAPOR ON A HORIZONTAL PLATE

by

Paul M. Meyrial
Michel L. Morin

Sponsored by

National Science Foundation
Contract No. GK-1113

March 1, 1968

Engineering Projects Laboratory
Department of Mechanical Engineering
Massachusetts Institute of Technology
Cambridge, Massachusetts
02139

ABSTRACT

The object of the investigation is to analyze the following two features of heat transfer during condensation of potassium vapor:

a. Heat transfer during film condensation of a pure saturated potassium vapor on a horizontal surface.

b. Heat transfer during film condensation of potassium vapor in the presence of a small quantity of non-condensable gas.

Until now, the discrepancy between theory and experiment concerning the condesnation of pure liquid-metal vapors has been explained by a thermal resistance at the liquid-vapor interface. This interfacial resistance was analyzed by means of the kinetic theory, and the results depended on the use of a condensation (or accommodation) coefficient. This coefficient was found to decrease in value at higher pressures.

This work presents a more refined analysis of the interfacial temperature distribution, including the effect of subcooling in the vapor in the region of the liquid-vapor interface.

Furthermore, a theory predicting the temperature drop in the condensate film on a horizontal plate is presented.

Experiments were performed to verify the theory. In addition, data from previous investigators were analyzed. Experiments with non-condensable gases in the saturated vapor were made using the horizontal plate facing upward. These results supported Kroger's (19) theory.

ACKNOWLEDGEMENT

This work was sponsored in part by the National Science Foundation under Contract No. GK 1113 and sponsored by the Division of Sponsored Research of M.I.T.

TABLE OF CONTENTS

TABLE OF CONTENTS (CONT.)

LIST OF TABLES

LIST OF FIGURES

LIST OF FIGURES (CONT.)

NOMENCLATURE

A	area and accomodation coefficient
B,C	constant
C_p	specific heat
D_{ij}	binary diffusion coefficient
D_i^T	thermal diffusion coefficient
d	thickness of the discontinuity zone
F	elliptic integral of the first kind
G	relation between mass flow rate and temperature drop in the film
g	gravitational acceleration
h	enthalpy or heat transfer coefficient
h_{fg}	latent heat of vaporization
J_u	energy flux
j	mass flux with respect to mass average velocity
K	Boltzmann constant
k	thermal conductivity
K_T	thermal diffusion ratio
L	half length plate
ℓ	length
M	molecular weight
m	mass per molecule
n	number density
p	pressure

NOMENCLATURE (CONT.)

q_c	condensation heat flux
R	universal gas constant
S	molecular cross section
s	variable
T	temperature
t	effective gas thickness
u	velocity in the film
$\bar{V}$	diffusion velocity
$\bar{v}$	average molecular velocity
v_o	mass average velocity
v_b	mole volume
v_{fg}	difference between vapor and liquid specific volume
W	mass flow rate per unit width and mass of non-condensable
w	mass flux
X_k	external force
x	coordinate
x^*	dimensionless coordinate
y	coordinate
z	dimensionless thickness
α	thermal diffusivity
β	constant
γ	ratio of specific heat

NOMENCLATURE (CONT.)

Γ	correction factor as defined by equation 4 (reference 19)
δ	thickness of the film
δ_o	thickness of the film at the center of the plate
ε_o	emissivity
ε/K	potential energy parameter
φ	parameter defined by Equation (d-5)
Λ	dimensionless parameter as defined by Equation (d-4)
λ	mean free path
μ	dynamic viscosity
ν	kinematic viscosity
$\Omega^{(22)}, \Omega^{(11)}$	collision integrals
ρ	density
σ	condensation coefficient
σ^*	Stefan-Boltzmann constant
τ	viscous stress
ξ	dimensionless parameter defined by Equation (d-3)
ζ	temperature jump coefficient

Subscripts

Av	average
b	boiling
c	critic and condensate
i	interface
i,j	i-th and j-th components

NOMENCLATURE (CONT.)

ℓ	distance
m	vapor-gas mixture
s	condensate surface
v	vapor
w	wall

INTRODUCTION

In recent years, liquid metals have become important as heat transfer media in nuclear reactors for conventional power plants and also in space power generating units. The high thermal conductivity and high temperature characteristics of liquid metal improve thermal efficiency, and their low vapor pressures permit the use of lighter and more compact units.

This work continues the investigation carried out by Kroger (19) on heat transfer during condensation of potassium vapor and the effect of the presence of traces of non-condensable gases on the heat transfer coefficient.

Review of the Literature

The first formulation of the problem is credited to Nusselt (1) whose analysis was later improved and refined by several investigators. Seban (2) presented an extension of Nusselt's theory for high Reynolds numbers. Broomley (3) studied the effect of subcooling of the condensate, and Rohsenow (4) derived an analysis for a non-linear temperature distribution in the film. By means of a similar transformation, Sparrow and Gregg (5) accounted for the momentum changes in the condensate film. Mabuchi (6) obtained the same results by an integral method.

The effect of the vapor drag has been studied by Chen (7), Koh, Sparrow and Harnett (8), Koh (9), and Chato (10).

A theoretical analysis, giving the thickness of the film in the case of condensation of saturated vapor on a horizontal plate facing upward, has recently been derived by Clifton and Chapman (11).

Experiments have been performed which verify the theoretical predictions for liquids with $Pr > 0.5$ (12). However, in the case of liquid metals, the experimental heat transfer coefficients were found to be much smaller (five to thirty times) than predicted by Nusselt. References (13), (14), (15), (16), (17), (18), and (19) show this trend.

Several explanations of this discrepancy had been given:

a. A resistance at the solid-liquid interface
b. A film thickness other than predicted by Nusselt
c. The presence of non-condensable gases
d. Impurities on the condensate surface
e. A resistance at the liquid-vapor interface.

The thermal resistance at the solid-liquid interface could be due to formation of oxide layers, adsorbed gases, or chemical reactions between the condensate and the wall. A good choice of the condensing plate material and a careful outgasing and cleaning of the system could eliminate such resistance.

As far as the film thickness is concerned, Sukhatme (16) verified that it does not vary substantially from Nusselt's prediction.

The third possible cause of the reduced heat transfer rate, that

is the presence of non-condensable gases, can be eliminated by continuous purging and a leak-tight system.

Impurities on the condensate surface are unlikely to occur in the condensation process. Consequently, the most probable cause of the lower heat transfer rate is the presence of a thermal resistance at the liquid-vapor interface. The nature of this resistance and the application of the modified Hertz-Knudsen equation for interphase mass transfer were analyzed in detail by Schrage (20). This problem was also studied by Wilhelm (21), Mills (22) and Barry (23).

A rigorous thermodynamics approach, though limited to low mass transfer rates, was presented by Bornhorst (24), whose results were later confirmed by Adt (25).

Using a combination of both Schrage and Bornhorst analyses, Kroger (19) carried out a more refined investigation of the problem.

The Schrage analysis is based upon the assumption that no heat transfer occurs by conduction between the vapor and the liquid. The thermal resistance at the interface, and thus the heat flux, was found to be dependent on a condensation coefficient which had to be determined experimentally. All the experimental results show that the condensation coefficient decreases with increasing pressure. Actually, no physical consideration is able to support this behavior of the condensation coefficient.

It is therefore reasonable to assume that the temperature of the vapor near the interface is lower than the measured saturation

temperature; the decrease in temperature would be due to heat conduction from the "hot" vapor to the "cold" liquid.

Wilhelm (21) formulated this idea in 1964. The idea was verified experimentally by Subbotin, Ivolnovsky and Sorokin (26).

Schrage (20) discusses the temperature jump coefficient. In addition, Kennard (27) and Present (28) introduce the interface transfer zone where discontinuities occur in the vapor.

The presence of non-condensable gases in the system generally reduces the heat transfer rate. The first study of this phenomena was made by Reynolds (29). The experiments of Othmer (30) showed that condensation heat transfer of steam can be reduced significantly by the presence of small quantities of air. This trend is confirmed by Langen (31), Reed and Noyes (32) for sodium and Sukhatme (16) for mercury.

The principal analytical investigations of this problem were made by Colburn (33) (34), Chilton (35), Nusselt (36) and Merkel (37). Various practical design procedures for condensers were proposed by Kern (38), Bras (39) and Cairns (40).

Sparrow (41) derived a theory, based on the conservation law which seems to be supported favorably by the experimental result for air-steam mixtures.

Considering a one-dimensional model in which saturated vapor diffuses through a non-condensable gas and condenses on a horizontal

surface, Kroger (19) derived an analysis which has proved to comply with experiments using a potassium-helium mixture.

The problem of the vertical condensing plate has been studied theoretically by Rose (42)

PART I

CONDENSATION OF A PURE SATURATED POTASSIUM VAPOR ON A HORIZONTAL PLATE

-1-ANALYTICAL CONSIDERATIONS

This analysis is aimed at predicting the heat flux during filmwise condensation of a pure saturated potassium vapor on a horizontal surface facing upward (as shown in Figure 1).

Starting from the same assumptions as in Nusselt's theory (43), an analysis relating the mass flow rate of condensation to the temperature drop in the film is developed.

Theory will be used to predict the actual temperature T_i of the vapor at the interface. Then, an expression for the heat flux of condensation will be derived from the Schrage (20) equation, in which T_i is taken as the vapor temperature, instead of the bulk temperature T_v.

-1-a-Temperature Distribution in the Condensate Film

The following assumptions are made:

1. The temperature T_w of the condensing surface is uniform.
2. The condensate flow is laminar, and therefore the viscous shear is expressed by
$$\tau = \mu \frac{\partial u}{\partial y}$$
3. The temperature distribution in the film is linear, and is given by
$$T = T_w + (T_s - T_w) \frac{y}{\delta}$$
4. The fluid properties are constant.
5. The shear at the liquid-vapor interface ($y = \delta$) and the

and the momentum change through the film are negligible. This leads to the following boundary condition

$$\left[\frac{\partial u}{\partial y}\right]_{y=\delta} = 0$$

where: τ - is the shear stress

μ - the dynamic viscosity

u - the velocity in the condensate fluid

T_w - the wall temperature

T_s - the temperature of the liquid at the interface

y - the direction perpendicular to the surface

The velocity distribution in the condensate film is derived from Newton's law applied to a volume element of liquid as shown in Appendix A.

Nelgecting the inertia forces, the balance of forces on the liquid element leads to the following differential equation:

$$\frac{\partial^2 u}{\partial y^2} = \frac{\rho g}{\mu} \frac{d\delta}{dx} \qquad \text{(a-1)}$$

with the boundary conditions:

at $y = 0$, $u = 0$

and at $y = \delta$, $\frac{\partial u}{\partial y} = 0$

The integration is readily obtained:

$$u = \frac{\rho g}{\mu} \delta^2 \frac{d\delta}{dx} \left[\frac{1}{2} \left(\frac{y}{\delta}\right)^2 - \frac{y}{\delta} \right] \qquad \text{(a-2)}$$

The mass flow rate per unit width, W, is then calculated as follows:

$$W = \rho \int_0^{\delta} u \, dy = - \frac{\rho^2 g}{3\mu} \delta^3 \frac{d\delta}{dx} \qquad \text{(a-3)}$$

Equating heat flux with enthalpy change:

$$\frac{q}{A} = k \frac{T_s - T_w}{\delta} = h'_{fg} \frac{dW}{dx} \qquad \text{(a-4)}$$

where h'_{fg} is the average enthalpy change of the vapor.(I)

Substituting in the value of W from equation a-3, the following differential equation in δ is obtained:

$$\delta^3(3\delta'^2 + \delta\delta'') = \frac{3k\mu}{\rho^2 g \, h'_{fg}} (T_s - T_w) \qquad \text{(a-5)}$$

It is not possible to integrate this equation directly; but using the dimensionless parameters x^*, z, ξ and Λ, defined by:

$$x^* = \frac{x}{L} \qquad \text{(d1)} \qquad\qquad z = \frac{\delta}{\delta_o} \qquad \text{(d2)}$$

$$\xi = \frac{T_s - T_w}{h'_{fg} (\mu/k)} \qquad \text{(d3)} \qquad\qquad \Lambda = \xi^{1/2} \left(\frac{\rho}{\delta_o}\right)^{5/2} \qquad \text{(d4)}$$

where L is the half length of the plate, δ_o is the thickness of the film at the center of the plate, and ρ is a constant. We can now write equation (5) as follows (Appendix B):

(I) This average enthalpy change includes the latent heat of condensation and the change of enthalpy due to the subcooling to the average liquid temperature.

$$z\sqrt{1 - z^3} + 1/3^{1/4} F = 5/2^{1/2} \; x^* \Lambda \qquad \text{(a-6)}$$

with $$\varphi = \left[\frac{\mu_L^2}{\rho^2 g}\right]^{1/5} \qquad \text{(d5)}$$

and where F is an elliptic integral of the first kind, the values of which are tabulated.

The thickness of the film at the plate's edge, called critical depth in the theory of open-channels, is, according to Clifton and Chapman (11):

$$\delta_c = \frac{54}{35} \left(\frac{W_c^2}{\rho^2 g}\right)^{1/3} \qquad \text{(a-7)}$$

This gives the following relation in terms of the parameters previously defined:

$$\left(\frac{\delta_o}{\varphi}\right)^5 = \frac{35/12}{\Lambda^2 \; \frac{1 - z_c^3}{z_c^4}} \qquad \text{(a-8)}$$

Equation (a-6) with condition (a-8) and the definitions (d-1,2,3,4,5) permit the computation of w as a function of $(T_s - T_w)$:

$$w = G(T_s - T_w) \qquad \text{(a-9)}$$

This function is plotted on Figure 4 and the details of the calculations can be found in Appendix C.

1-b Temperature Distribution in the Vapor

As shown in Figure 1, the present situation is as follows:

A saturated potassium vapor at uniform bulk temperature, T_v, is in contact with the liquid film whose surface temperature T_s is lower than T_v.

Therefore, heat transfer occurs from the vapor to the liquid, and a non-zero temperature gradient exists in the vapor near the interface.

Furthermore, as suggested by many investigators, Langmuir (45), Fowler (46), Chapman and Cowling (47) and confirmed by the kinetic theory, the interface between a liquid and a gas presents a layer of transition in which the properties of the phases are not uniform.

The thickness of this layer depends on the vapor and liquid properties and can be expressed as a function of the mean free path λ of the vapor molecules.

The thermal discontinuities occurring at the interface can be expressed by means of the temperature jump coefficient ζ defined by the equation

$$T_i - T_s = (\zeta + d) \left[\frac{dT}{dx}\right]_i \qquad \text{(b-1)}$$

where (see Figure 3) T_i is the actual temperature of the subcooled vapor molecules striking the liquid surface, T_s is the temperature of the liquid at the interface, $\left[\frac{dT}{dx}\right]_i$ is the temperature gradient of the vapor at the interface and d is the thickness of the transfer zone.

Considering the magnitude of d, the condensation process occurring in the transfer zone can be treated as a "rarefied gas" problem and the temperature jump coefficient is expressed by

$$\zeta = \frac{2}{Pr} \frac{2-A}{A} \frac{\gamma}{\gamma+1} \lambda \qquad \text{(b-2)}$$

where Pr is the Prandtl number of the vapor

A is the thermal accommodation coefficient

γ is the ratio of specific heats

No precise data are available concerning the magnitude of d, but the slip theory for a gas in contact with a solid surface shows that the average distance of the molecules striking the surface equals two thirds of the mean free path of the molecules (43).

However, in the condensation process, the presence of a mass transfer and of a liquid (instead of solid) wall is likely to alter this value. According to Present (28) and Kominsky (48), the magnitude of d could reach "several" mean free paths. Le Febvre (49) evaluates it from 1 to 5λ. This investigation takes account of three different values of d: λ , 3λ , 10λ .

The thermal accommodation coefficient will be taken equal to one; this assumption will be justified a posteriori by the finding that the condensation coefficient σ equals one.

In addition to Equation b-1, the energy balance on a control volume in the vapor as shown in Figure 3, gives a relation between

T_i and $[\frac{dT}{dx}]_i$:

$$w\, c_p\, (T_v - T_i) = k_v [\frac{dT}{dx}]_i \qquad \text{(b-3)}$$

where w is the condensation mass flux, c_p is the specific heat of the vapor and k_v the thermal conductivity of the vapor.

The expression from which T_i can be calculated is directly derived from Equation b-1 and b-3:

$$\frac{T_v - T_i}{T_i - T_s} = \frac{k_v}{w\, c_p (\zeta + d)} \qquad \text{(b-4)}$$

1-c Condensation Heat Flux

At the interface, the liquid is at the temperature T_s calculated from the film analysis and at pressure p_s, saturation pressure corresponding to T_s; the vapor is at temperature T_i calculated from Equation b-4 and at saturation pressure p_i corresponding to T_i. The saturation conditions are assumed at the interface since only the slightly non-equilibrium cases are treated here, that is:

$$\frac{p_v - p_s}{p_s} \ll 1$$

Therefore, according to Kroger (19), the Schrage equation for interphase mass transfer gives in case of small departures from equilibrium:

$$w = \frac{2\sigma}{2-\sigma} \left(\frac{M}{2\pi R}\right)^{1/2} \left(\frac{p_s}{T_s^{1/2}} - \frac{p_i}{T_i^{1/2}}\right) \qquad \text{(c-1)}$$

where M is the atomic weight, R is the universal constant and σ is the condensation coefficient defined as the ratio of the number of vapor molecules condensing over the total number of molecules which strikes the surface.

For most cases, $\frac{T_i - T_s}{T_s} \ll \frac{p_i - p_s}{p_o}$ and Equation c-1 may be simplified to read:

$$w = \frac{2\sigma}{2-\sigma} \left(\frac{M}{2\pi R T_i}\right)^{1/2} (p_s - p_i) \qquad \text{(c-2)}$$

In the present investigation, q_c, T_v, and T_w are determined experimentally, and the following set of equations permits one to calculate the four unknowns w, T_s or p_s, T_i or p_i, and particularly σ:

$$q_c = -w\, h'_{fg} \qquad \text{(c-3)}$$

$$w = G(T_s - T_w) \qquad \text{(a-9)}$$

$$\frac{T_v - T_i}{T_i - T_s} = \frac{k_v}{w\, c_p (\zeta + d)} \qquad \text{(b-4)}$$

and

$$w = \frac{2\sigma}{2-\sigma} \left(\frac{M}{2\pi R T_i}\right)^{1/2} (p_s - p_i) \qquad \text{(c-1)}$$

For design purpose, where T_v and T_w are given, the knowledge of σ will permit one to predict the condensation heat flux q_c by means of the same equations.

It is noted that, in the situations where the Nusselt film analysis applies, the condensation heat flux would be calculated from Equations b-4, c-1, c-2 and the Nusselt equation

$$q_c = 0.943\sqrt[4]{\frac{g\rho(\rho_\ell - \rho_v)k^3 h'_{fg}}{\ell\mu}}\,(T_s - T_w)^{3/4}$$

2 DESCRIPTION OF THE EQUIPMENT

2-a-Summary

The general scheme of the apparatus, shown in Figure 9, is identical in its principle to Kroger's apparatus (19). However, major components have been modified. The condensing surface is horizontal.

In these experiments, low sodium grade potassium has been used.

The potassium can be transferred from its container to the boiler through a heated transfer line. The boiler is overtopped by the condensing unit. The latter is connected via a heated exhaust line and a condenser to a mechanical vacuum pump. At the bottom of the condenser, the temperature of the condensate is controlled, allowing a re-circulation of the potassium in the transfer line. Both boiler and condensing unit can be evacuated or pressurized with an inert gas. A scintillation counter and a radioactive source are used to detect the level of the liquid metal surface in the boiler. The cooling of the condensing plate is realized by a circulation of silicone oil.

All joints in the boiler-condensing unit-condenser were heliarc welded to avoid leaks. The absolute tightness of the system was checked before each experiment. After evacuating the system the absence of leaks was verified over a period of 24 hours.

2-b-Major Components

The main components of the equipment are described below.

Boiler:

The boiler mainly consists of a 10 inch nominal stainless steel 316 pipe welded with a reducer leading to a 6 inch I.D. x 13 inch long cylinder in which a superheater can be placed. The boiler is ended with a 0.75 inch thick base plate at the bottom. The upper end is fitted with a flange to which the condensing unit is welded. Thirty two 0.84 inch O.D. holes for heating elements sheaths are located in the pipe section. The 4 inch long radial sheaths contain Watlow firerod cartridge heating elements as shown in Figure 13. An outer cylindrical jacket of stainless steel, having the dimensions of 20 inch O.D. x 28 inch long, surrounds the boiler section and is bolted on two flanges at the top and the bottom. The space between the jacket and the system is filled with insulating material and can be either evacuated or pressurized with an inert gas, preventing oxidation of the outer boiler surface at high temperatures. The boiler with lowered jacket is shown in Figure 14.

Three probes were installed in the boiler, each containing a thermocouple for measuring the liquid temperature and the vapor temperature at two different levels.

Condensing Unit

The vertical walls of the condensing unit consist of a portion of a 7 inch O.D. 10.25 inch long stainless steel cylinder welded to a flat surface. At the bottom, a 12.5 inch O.D. flange matches the upper part of the boiler. The vapor is evacuated at the top through

a 1.25 inch O.D. stainless steel pipe welded to the cover plate. Potassium vapor is condensed on a square (3in x 3in) horizontal stainless steel 304 plate, 0.875 inches thick as pictured in Figure 12. Seven, 0.063 inch diameter holes are located in the plate, containing the ceramic shields of the thermocouples. Three thermocouples give the temperature distribution at the center of the plate, whereas the thermocouples located in each corner give the temperature distortions. The cooling fluid (silicone oil) circulates under the condensing plate in a square box, fitted with three fins. A lateral insulation prevents the heat transfer between the cooling box and the vapor. The condensing plate is surrounded on the top by three 1.5 inch high stainless steel walls to avoid convective motions. The condensate is allowed to flow off the plate's edges through small clearances, 0.13 inches high. Both condensing surface and cooling box are welded to the vertical flat wall of the condensing unit. An external resistance heater compensates for the heat losses to the surroundings during the run. The entire unit is wrapped in an insulating material (cerafelt CRF 800) and enclosed in a vacuum-tight outer jacket that can be filled with an inert gas during operation to prevent oxidation.

Condenser:

The condenser consists of three distinct adjacent chambers, realized with two coaxial stainless steel cylinders respectively of 2.5 inches I.D. and 5 inches I.D. The annular space is divided

in two parts by a partition welded on both cylinders. The various parts are shown in Figure 11. The first chamber is 12 inches long and is connected via a heated 1.25 inch diameter stainless steel pipe and a stainless steel valve to the condensing unit. The second and third chambers, 24 inches long, are cooled down at the top by a cooling coil.

The condensate is collected at the bottom of the first and second chambers; its temperature is controlled by a resistance heater and it can be recirculated through a 1 inch diameter pipe in the transfer line. The 0.37 inch diameter vacuum line is welded to the wall of the third chamber.

Cooling System:

A drawing presenting the major components of this system is shown in Figure 15. Dow Corning 200 Fluid silicone liquid is used as a coolant. Chemically inert, it undergoes a very slight change of properties over a wide temperature span, and is serviceable to over 600 F. The plumbing is realized in 1 inch diameter copper pipes silver soldered. The desired flow rate is insured by a pump, controlled by a by-pass, and measured by a flowrator meter type 10 A 2700 Fischer and Porter. The calibration curve for liquid density 1.0 can be used with a correction factor 1.09. After cooling of the condensing surface, the liquid passes through a water heat exchanger. Two thermocouples give the temperature at the inlet and outlet of the condensing unit.

Potassium Fill System:

Low sodium grade potassium (25 lbs.) is stored in a standard shipping container constructed of stainless steel and equipped with necessary piping and valves to permit transfer under pressure of inert cover gas. The container is heated with two narrow banded Watlow heaters of 3.75 KW output each to melt potassium before transfer. A stainless steel line, connected with a bottle of inert gas (Helium or Argon) is attached to the inert gas port. It contains provisions for both vacuum and cover gas. The discharge line is connected to the boiler with a stainless steel transfer line.

The latter is heated by a Glas-Col laboratory type heating tape, consisting of parallel heating ribbons encased in silicone rubber and giving a temperature up to 480^{o}F.

Control and Measurements:

Temperature

The following temperatures were measured:

- temperature of the liquid metal in the boiler
- temperature of the vapor in the boiler
- temperature of the vapor in the condensing unit at four locations above the condensing surface
- temperature of the condensing unit walls
- temperatures in the condensing surface at seven locations
- temperature of the cooling fluid at the inlet and outlet
- temperature of the vapor in the condenser at five locations

- temperature of the container

All temperatures are measured by means of Chromel-Alumel thermocouples. Conax thermocouples insulated with magnesium oxide and shielded with inconel are used to read the temperatures inside the system. These thermocouples are inserted in stainless steel probes welded to the walls. The thermocouples are connected, via two Leeds and Northrup multipole rotary switches, to a Leeds and Northrup precision potentiometer capable of reading to within 0.01 millivolt.

Power and Currents:

The three phase mains supply 220 volts to a variable voltage transformer having a maximum output of 18 KW. Five switches and five ampmeters control the network feeding the heating system of the boiler. Twenty-one Watlow firerod cartridge heating units are connected as indicated in Figure 16 to supply a maximum output of 9.75 KW. The power output of the compensating resistance heater attached to the condensing unit and the power required for the heating of the reservoir are controlled by separate variacs and ampmeters. 115 volts laboratory power was used for the heating tapes and the pumps.

The system control panel is shown in Figure 10.

Detection of the Liquid Metal Surface Level in the Boiler:

The level of the potassium in the boiler is detected by means

of a gamma ray attenuation technique. A schematic diagram of the equipment is given in Figure 17. The radio-active source received in solid form on a thin rod is inserted in a lead container. The latter is mounted on a vertically adjustable support next to the boiler section. Gamma radiation is beamed through the walls of the system. A scintillation counter (Model 10-8) protected by a lead shield is mounted on the same support, in line with the source and diametrically opposite from it. The gamma beam enters through a 3/8 inch diameter hole drilled in the shielding. The scintillation counter consists essentially of a scintillation crystal, a photo-multiplier tube and a pre-amplifier. The high voltage is provided by a M.V. power supply (Model 40-8B) in a range of 395 through 1350 volts. The output of the pre-amplifier was fed into a linear amplifier and discriminator (Model 30-19) before being counted on a seven decade electro-mechanical scaler (Model 49-30). All these instruments were provided by the Radiation Instrument Development Laboratory, and are inserted into a standard instrument case (Model 29.1)

The strength of the source was determined in order to have a large count rate with respect to the background count, when there is no potassium in the boiler. When the level of the liquid metal rises, such that it intercepts the beam, there is a drop in the count rate.

Containment and Safety Control:

The parts of the system in which the potassium is boiled and condensed is entirely made of stainless steel and is essentially an all-welded construction. In addition, the vacuum tight jacket portects against possible liquid metal leakage. The tubing is assembled with Swagelok fittings and can be closed by Hoke stainless steel sealed bellows valves. Safety equipment includes two extinguishers "Fyr-Fyter" containing a dry chemical, safety helmets, safety glasses, and leather gloves (Mine Safety Appliance).

In order to safely operate the apparatus, an automatic temperature control is utilized as shown in Figure 16. A Fenwal Thermoswitch monitors the temperature of the boiler. In case of overheating of the system, this device activates a magnetic contractor and all power is immediately shut off.

3 EXPERIMENTAL PROCEDURE

The following operations were made:

1. Cleaning of the System

In order to remove oxides, grease and other impurities, the system was first flushed with a solution of hydrochloric acid and then rinsed several times with distilled water. It was then filled with trichlorethylene (a degreaser) and rinsed again with water. Finally, the system was flushed with acetone.

At this stage, the system was dried and outgased by evacuating at about 700°F. All connections, pipes and fittings were leak checked.

2. Transfer of Potassium

The supply tank of potassium was slowly heated to about 500°F. The transfer line and the boiler were also maintained at this temperature.

Then by pressurizing the reservoir at about 20 psia and keeping the remaining system evacuated, the potassium was transferred to the boiler until the potassium intercepted the gamma ray located at the desired operating level. This level corresponds to about 20 pounds of potassium in the boiler.

3. Run of a Test

The potassium was slowly heated while the system was evacuated.

At about 800°F, first boiling occurred. The exhaust valve was then closed. By increasing the power input, the vapor temperature of potassium was increased to 1400°F. The system was then evacuated again. The de-gassing operation was repeated several times. During the entire process, the condensation surface was not cooled. Condensation occurred only in the condenser outside the system. The purpose of these purges without condensation in the system was to eliminate the non-condensable gases.

The condensing surface was then cooled by circulating silicon oil.

Both the heating power in the boiler and the cooling flow rate had to be adjusted to obtain a steady state. The steady state was indicated by consistent reading of five thermocouples in the vapor, seven thermocouples in the condensing plate and three thermocouples in the side walls of the condensing unit.

The liquid temperature, the oil temperature at the inlet and outlet, together with its flow rate, were read. Then the power input was increased, and the system purged again while the cooling of the condensing plate was stopped.

At this stage, the purge valve was closed and the cooling flow was adjusted for another run.

The vapor temperature was measured by means of five thermocouples located at 1/4 in., 3/4 in., 1/2 in., and 4 in. from the condensing

surface and above the boiling surface.

The temperature gradient in the condensing plate was measured by three thermocouples. In addition, four thermocouples were located at the corners of the plate to evaluate the lateral heat losses.

4 EXPERIMENTAL RESULTS

The main purpose of this investigation was the determination of the condensation coefficient σ using Equations (a-9), (b-4), (c-1) and (c-2). The parameters q_c, T_w and T_v must be known.

The condensation heat flux q_c was determined by the temperature gradient in the condensing wall. A set of three thermocouples located in the center indicated the gradient itself. The heat losses on the sides were evaluated by means of four thermocouples located at the edges of the plate. These losses were found to be negligible.

The reading of the flux was checked by reading the inlet and outlet temperatures of the cooling fluid. In addition, a flowmeter indicated the flow rate of coolant.

The physical properties of the coolant, a mixture of two centistoke and five centistoke silicon oil "200 Fluid", were provided by the Dow-Corning Company.

These two heat flux readings were found to be consistent; however, it must be mentioned that the readings of low coolent flow rates were found to be inaccurate

The data on stainless steel thermal conductivity versus temperature was taken from the A.S.M.E. Handbook (50).

The wall temperature was obtained by extrapolation of the temperature distribution in the plate. An error of 0.5 to $1^{o}F$ was recorded due to the slight non-linearity of the temperature distribution in the

wall.

The vapor temperature was measured by means of five thermocouples located above the condensing surface and in the boiling region. The readings of these probes were consistent with each other.

The corresponding saturation pressure was calculated from an expression derived by Lemmon et al. (51).

$$\log_{10} p = 4.185 - \frac{7797.6}{T} \qquad (4.1)$$

where p is in atmospheres and T is in degrees Rankin.

The physical properties for potassium were found in Weatherford (52), with the exception of thermal conductivity for which more reliable data were given by Stephanov, Timrof and Totzki (53).

The temperature T_s was calculated from the values of T_w and the flux q_c using the relation $W = G(T_s - T_w)$ plotted in Figure 4. It was necessary to correct these theoretical results with a correction factor to account for the differences of geometry between the theoretical and the actual condensing surface. This coefficient was determined experimentally and its average value for the range of flow rates used here was 0.8.

The mean free path λ was calculated from the usual expression,

$$\lambda = \frac{1}{\sqrt{2}\, S(T) n} \qquad (4.2)$$

where n is the number density and S(T) is the cross section of the vapor molecules whose expression is presented by Hirschfelder, Curtiss, and Bird (54).

$$S(T) = 266.93 \frac{\sqrt{MT}}{\mu 10^7} \qquad (4.3)$$

where M is the atomic weight, T is the temperature in degree Kelvin, μ is the kinematic viscosity in poises and S(T) is expressed in square Angstroem.

The effect of dimerization was neglected. As shown by Kroger (19), the mole fraction of dimer to vapor is below 0.055 for the present experiments.

The tests were carried out with temperatures ranging from 825 to 1270°F. The heat flux varied from 46,000 to 120,000 Btu/hr ft^2 as shown in Table 3.

Figure 6a represents the condensation coefficient as a function of the thermodynamic state of the liquid surface for three different values of the transfer zone thickness d. The results scattered about constant straight lines. This is due to the error in the calculation of pressures. The probable error on σ is shown in Figure 6-b.

However, Figure 6-a shows that σ is independent of the vapor pressure. In addition, if the value of the transfer zone thickness, d, is taken equal to 3λ the values of σ are close to one.

A sample of calculation of σ is given in Appendix D. Figures 7-a,b,c show the results of other investigators whose data have been reworked according to the theory developed in this work. All the results show that the condensation coefficient is constant, and close to one. A discrepancy should be noted for the data from Barry (23) which lay significantly below one.

PART II

THE EFFECT OF A NON-CONDENSABLE GAS ON THE HEAT TRANSFER RATE DURING CONDENSATION OF POTASSIUM VAPOR

5 ANALYTICAL CONSIDERATIONS

The analysis predicing the heat flux during condensation of potassium vapor containing a known amount of non-condensable gas was developed by Kroger (19). This work states the main findings of Kroger's theory and applies them to the condensation of potassium vapor on a horizontal surface facing upward. The horizontal system was designed to avoid the convective motions occurring near the surface, as shown in Figure 12.

The geometry of the system allows one to use a one-dimensional model as shown in Figure 18 in which saturated potassium vapor diffuses through a non-condensable gas and condenses at the surface. Pure vapor exists at the distance ℓ from the condensing surface.

Hirschfelder and Curtiss (54) give the expression for the energy flux per unit area through a surface fixed with respect to the condensing surface:

$$Ju = -k_m \frac{dT}{dy} + \sum_{i=1}^{\nu} h_i n_i m_i (\bar{V}_i + v_o) + \frac{KT}{n} \sum_{i=1}^{\nu} \sum_{\substack{j \\ j \neq i}} \frac{n_j D_i^T}{m_i D_{ij}} (\bar{V}_i - \bar{V}_j) \tag{6-1}$$

where k_m is the thermal conductivity of the mixture, D_{ij} and D_i^T are the binary diffusion and thermal diffusion coefficient respectively, h_i is the enthalpy per unit mass of the i^{th} component, K is the Boltzmann constant, n_i, n_j and n are the number densities of the components and the mixture respectively, v_o is the mass average velocity, m_i is the mass of the i^{th} particle, and $\bar{V}_i$ and $\bar{V}_j$ are the

diffusion velocities of components i and j.

In the present two-component system, subscripts 1 and 2 will refer respectively to the potassium vapor and the gas.

Equation 6-1) represents the energy transported through the mixture by three different processes, respectively: heat conduction, enthalpy flux and thermal diffusion flux.

Expressing the diffusion velocities in terms of the thermodynamic properties and the reciprocal binary diffusion coefficient of the components, Kroger (19) derives the expression for the energy flux:

$$Ju = -[k_m + \frac{pk_T\beta}{T}] \frac{dT}{dy} - \beta \frac{dp_1}{dy} \tag{6-2}$$

where $$\beta = \frac{pD_{12}}{(p-p_1)} [\frac{h_1 M_1}{RT} + \frac{k_T p}{p_1}] ,$$

k_T, known as the thermal diffusion ratio, is defined by

$$k_T = \frac{\rho}{n^2 m_1 m_2} \frac{D_1^T}{D_{12}} \tag{6-3}$$

p_1 is the partial pressure of the vapor, p the pressure of the mixture, and ρ the mass density.

The mass conservation equation for the vapor gives another expression relating p_1 and T:

$$w = m_1 n_1 \bar{v}_1 = m_1 n_1 \bar{V}_1 + m_1 n_1 v_0 \tag{6-4}$$

Substituting the expressions of $\bar{v}_1$, $\bar{V}_1$, and $\bar{v}_0$, and introducing k_T, one finds:

$$w = \frac{- D_{12} M_1 p}{RT(p-p_1)} \left[\frac{dp_1}{dy} + \frac{k_T p}{T} \frac{dT}{dy}\right] \tag{6-5}$$

The temperature and vapor partial pressure distributions can be obtained if Equations (6-2) and (6-5) are solved numerically.

The condensation heat transfer is

$$q_c = -w[h_{fg} + C_p(T_\ell - T_o)] \tag{6-6}$$

where h_{fg} is the latent heat of vaporization and C_p the specific heat. The drop of temperature in the film and the interfacial resistance are small compared with $(T_\ell - T_o)$ and are neglected in the present analysis.

The procedure for calculating q_c is by trial and error. (Given an arbitrary value of w, substitute in (6-5) and solve for the temperature distribution with boundary conditions T_o and T_ℓ and the pressure distribution with boundary conditions $p_1 = p$ at $y = \ell$ and p_{10}, the saturation pressure, corresponding to T_o at $y = 0$.)

Then, from the partial pressure of the gas, it is possible to calculate the mass W of the gas. This value of W is compared with the measured value. If agreement is not obtained, another value of w is chosen. The calculation is repeated until the calculated and the measured values of W coincide.

q_c is then obtained from Equation (6-6).

For engineering purposes, where the temperature gradients are modest, the effect of thermal diffusion is negligible, that is

$$\frac{k_T p}{T} \frac{dT}{dp_1} \ll 1$$

and the mass diffusion equation becomes

$$w = \frac{D_{12} M_1 p}{RT(p-p_1)} \frac{dp_1}{dy} \tag{6-7}$$

where

$$D_{12} = \frac{CT^{3/2}}{dy}$$

and C = 0.348 for K-He and 0.091 for K-A .

By assuming that the gas is at average pressure p_{2m} , defined as

$$p_{2m} = - (p-p_{10}) \frac{M_1 CT_{av}^{1/2}}{wR\ell} \tag{6-8}$$

where $$T_{av} = \frac{T_\ell + T_o}{2}$$

Kroger (19) introduces the effective thickness of gas t defined as:

$$t = \frac{p_{2m}}{p} \ell \tag{6-9}$$

Substitute this equation in 6-8 and find

$$w = - \frac{(p-p_{10}) M_1 CT_{av}^{1/2}}{pRt} \tag{6-10}$$

The condensation heat flux is given by Equation (6-6).

The condensation heat transfer is finally expressed as:

$$h_c = \frac{p-p_{10}}{p} \frac{M_1 C T_{av}}{tR(T_\ell - T_0)}^{1/2} [h_{fg} + C_p(T_\ell - T_0)] \qquad (6\text{-}11)$$

The approximate method is used in the present experiment since the difference between the values of $q_{c\ \text{exact}}$ and $q_{c\ \text{approximate}}$ does not exceed 6%.

6 EXPERIMENTS AND RESULTS

6-1-Equipment

The apparatus used for this work consisted of the same equipment as described in Section 2.

In addition a non-condensable gas supply line was connected to the boiler. This line was composed of a molecular sieve bed, containing pellets at liquid Nitrogen temperature through which the gas was dried and purified. The second main component was the gas volume measuring device shown in Figure 20. The displacement method was used to control the desired volume of gas to be introduced into the system.

With valve 2 closed, valve 1 was opened. The gas which was under pressure displaced the mercury. Valve 1 was then closed and valve 2 was opened slowly in order to let the desired amount of gas into the system. The volume and the pressure of the gas were read directly from the drop of the mercury level in the 50 cm^3 buret.

6-2-Procedure - Experimental Results

For the present series of experiments, the procedure was very similar to the one described in Section 3. The system was allowed to reach a state of stable boiling and condensation. The introduction of the gas was then performed following the process described above.

Once the gas was introduced and the system had reached the steady state, the thermocouples in the vapor and in the condensing

plate were read several times. The thermocouples in the walls were also read as a check.

From the analysis developed in Section 5, the temperature of the pure vapor T_ℓ, the temperature at the interface T_o and the quantity of non-condensable gas W must be known in order to calculate the condensation heat flux q_c.

The value of q_c is also given experimentally by the gradient in the condensing plate. The comparison of these two values is shown in Tables 8 and 9 and in Figure 21.

The pressure p is the saturation pressure corresponding to T_ℓ since all the non-condensable gas is concentrated near the surface. Consequently, p was calculated from Equation 4.1.

The temperature distribution in the vapor was measured by means of four thermocouples located respectively 1/4 inch, 3/4 inch, 1 1/2 inches and 4 inches from the condensing surface. An example of such a distribution with the corresponding pressure distribution is shown in Figure 22.

The large difference in temperature between T_o and T_ℓ made it necessary to calculate the radiative heat transfer q_r between the walls and the condensing surface. The evaluation of q_r is shown in Appendix E. Its influence varies from 1 to 15% of the measured heat flux.

The theoretical condensation heat transfer coefficient was cal-

culated from Equation (6.11) using the approximate method. Kroger (19) showed that the results are not expected to vary substantially from those obtained with the exact method.

In the present experiments $\frac{k_T p}{T} \frac{dT}{dp}$ is negligible compared with 1.

Problems:

During the experimental investigation some difficulties were encountered.

First, the temperature distribution in the condensing surface was non-linear, making the evaluation of the heat flux and the wall temperature rather inaccurate. This was probably due to the difficulty of obtaining a steady state. Bumps were observed in the system while the temperature readings showed large fluctuations. These fluctuations, however, smoothed down with time and finally vanished.

An average gradient in the plate between the two thermocouples closest to the condensate surface was taken to measure the heat flux.

The second difficulty was due to the inadequacy of the condenser used at this time to evacuate non-condensable gases from the system. It resulted in frequent plugging of the exhaust line. In addition, a small amount of gas probably remained in the system after evacuation.

Finally, the insurance that condensation occurred only at the cooled surface was not established. As a matter of fact, the vapor could have condensed on other parts of the system. Consequently,

all of the gas might not have been above the test surface.

These uncertainties are sufficient to explain the discrepancy in the results between theory and experiment (Figure 22). As stated by Kroger (19), these discrepancies tend to increase for lower heat transfer coefficients.

The geometry of the surface was correctly designed since the convective motions mentioned by Kroger (19) in the case of addition of Argon were suppressed. This statement is deducted from the fact that experiments with both Helium and Argon are consistent with each other.

DISCUSSION AND CONCLUSIONS

7 DISCUSSION OF RESULTS

Condensation of Pure Vapor

The film analysis was based upon the following assumptions:

1. The temperature T_w of the condensing plate is uniform
2. The condensate flow is laminar
3. The temperature distribution in the film is linear
4. The fluid properties are constant
5. The shear at the liquid-vapor interface and the momentum change through the film are negligible

The uniformity of temperature on the surface of the condensing plate was not completely realized experimentally, since the cooling rate was not uniform throughout the plate. However, the temperature difference is small (about 3%) and does not significantly affect the film. The temperature at the center of the plate was taken as wall temperature.

The condensate flow is laminar since the Reynolds number is lower than 3000.

The linearity of temperature distribution in the film is a good approximation, for the conductive term in the energy equation is much more significant than the convective and dissipative terms (two thousand and two hundred times as much respectively).

The fluid properties in the film can be taken as constant since the variation of temperature in the film does not exceed $3^{\circ}F$.

Finally, it was shown in Appendix A that inertia terms can be neglected in the momentum equation.

The determination of the correction factor between the theoretical and the actual plate geometries was determined experimentally. A simulation of condensation process was realized with water whose properties are close to the properties of liquid potassium. The thickness of the film was measured for both geometries with different flow rates of condensation. An average value of the correction factor was taken for the calculations.

As far as the subcooling of the vapor is concerned, the assumption of heat conduction from the vapor to the liquid is justified by the temperature difference between the two media. The slip theory used to evaluate the temperature jump coefficient is valid for a solid surface in contact with a "rarefied gas".

The assumption of "rarefied gas" situation is supported by the nature of the discontinuity zone whose size is of the order of the mean free path of the vapor molecules. The same kind of situation occurs in shock wave phenomena (58). The situation of a fluid wall in contact with a gas has not been studied as yet, and no data are available for this purpose.

A lack of information and knowledge about the exact nature of the aforementioned discontinuity zone leads to a large uncertainty concerning the thickness d of this zone. This work presents data for several values of d. The latter are plotted on Figures 7a, b, c

suggesting for the thickness a number of mean free paths ranging between three and five.

The use of the saturation pressure corresponding to the temperature T_i at the interface is supported by the former assumption of a quasi-equilibrium situation made in order to derive Equation (c-1).

The validity of (c-1) was discussed in detail by Kroger (19) and is applicable in situations where:

$$\frac{p_v - p_s}{p_s} < 0.25$$

This investigation shows that a correct choice for the thickness d of the discontinuity zone brings all the data concerning the condensation coefficient σ around 1 independently of the value of the saturation pressure.

However, the condensation coefficient σ seems to be lightly influenced by the heat flux though no obvious relationship is involved.

Condensation in presence of a non-condensable gas.

The validity of the diffusion analysis was discussed by Kroger (19). As mentioned in section 6, the experimental results agree with this theory. This is despite all the experimental uncertainties previously described.

8 CONCLUSIONS AND RECOMMENDATIONS

For practical purposes, expression (c-2) is the most convenient to calculate the condensation heat flux. The condensation coefficient should be taken as unity while T_i and p_i are to be calculated from Equation (b-4) with $d = 5\lambda$.

However, further refinements have to be brought to the present theory.

The temperature jump coefficient should be investigated in the particular case of a gaseous medium in contact with a liquid wall. A deeper knowledge of the transfer zone would be of value in order to calculate the size of this zone and to determine the parameters which influence it. Kinetic theory and quantum mechanics might solve the problem.

Finally, experiments should be performed aiming at studying the behavior of the condensation coefficient when the heat flux varies for a fixed value of the vapor temperature.

In the case where a non-condensable gas is present in the system, the difficulties encountered by Kroger (19) were overcome by changing the geometry of the condensing element. When using a horizontal surface facing upward and applying Kroger's analysis, experiments and theory agree for both Helium and Argon within the same range of error. This would tend to prove that the convective motions, significant for a heavy gas, were responsible for the aforementioned difficulties.

As suggested by Kroger (19), it might be of considerable value to study the role of electrical surface charges during condensation process.

REFERENCES

1. Nusselt, W., Zeitsch. d. Ver. deutsch. Ing., 60, 541 (1916).

2. Seban, R.A., Trans. ASME, 76, 299, (1954).

3. Bromley, L.A., Ind. and Eng. Chem., 44, 2966 (1952).

4. Rohsenow, W.M., Trans. ASME, 78, 1645, (1956).

5. Sparrow, E.M. and Gregg, J.L., Trans. ASME, Series C, 81, 13, (1959).

6. Mabuchi, I., Trnas. Japan Soc. Mech. Engrs., 26, 1134, (1960).

7. Chen, M.M., Trans. ASME, Series C, 83, 48, (1961).

8. Koh, C.Y., Sparrow, E.M., and Hartnett, J.P., Int. J. Heat and Mass Transfer, 2, 79, (1961).

9. Koh, C.Y., Trans. ASME, Series C, 83, 359, (1961).

10. Chato, J.C., ASHRAE Journal, 4 (2), 52, (1962).

11. Clifton, J.V. and Chapman, A.J., ASME Publication 67 WA/HT18 (1967).

12. McAdams, W.H., "Heat Transmission", McGraw-Hill, (1954).

13. Misra, B. and Bonilla, C.F., Chem. Eng. Prog. Sym., Series 18, 52, 7, (1956).

14. Cohn, P.D., M.S. Thesis, Oregon State College, (1960).

15. Roth, J.A., Report ASD-TDR-62-738, Wright-Patterson AFB, (1962).

16. Sukhatme, S.P., Ph.D. Thesis, M.I.T., (1964).

17. General Electric Co., Qtr. Report 9, Ctr. NAS 3-2528, Oct. 1964.

18. Subbotin, V.I., Ivanovsky, M.N., Sorokin, V.P.. amd Chulkov, V.A., Teplofizika vysokih temperatur, No. 4, (1964).

19. Kroger, D.G., Sc.D. thesis, M.I.T. (1966).

20. Schrage, R.W., "A Theoretical Study of Interphase Mass Transfer", Columbia University Press, New York, (1953).

REFERENCES (CONT.)

21. Wilhelm, D.J., Ph.D. Thesis, Ohio State University, (1964).

22. Mills, A.F. and Seban, The Condensation Coefficient of Water, Int. Jour. of Heat & Mass Transfer, Vol. 10, No.12 (Dec. 1967).

23. Barry, R.E., Ph.D. Thesis, University of Michigan, (1965).

24. Bornhorst, W.J., Ph.D. Thesis, M.I.T., (1966).

25. Adt, R.R., Ph.D. Thesis, M.I.T. (1967).

26. Subbottin, V.I., Ivanovsky, M.N., Sorokin, V. P., Proceedings of Heat-Mass Transfer Conference, Minsk, 1966.

27. Kennard, E.H., "Kinetic Theory of Gases", McGraw-Hill (1938).

28. Present, R.D., "Kinetic Theory of Gases", McGraw-Hill (1958).

29. Reynolds, O., Proc. Roy. Soc., 144, (1873).

30. Othmer, D.F., Ind. Eng. Chem., 21, (1929).

31. Langen, E., Forschung a.d. Geb. d Ingenieurwes. 2, 359, (1931).

32. Reed, G.I., and Noyes, R.C., AEC Research and Development Report, NAA-SR-7325.

33. Colburn, A.P., Trans. AIChE, 29, 174, (1933).

34. Colburn, A.P., and Hougen, O.A., Ind. Eng. Chem. 26, 1178 (1934).

35. Chilton, T.H. and Colburn, A.P., Ind. Eng. Chem., 26, 1183, (1934).

36. Nusselt, W.A., angew. Math. Mech., 10, (1930).

37. Merkel, F.Z., Ver. dtsch. Ing., 72 (10), 342 (abstract), (1928).

38. Kern, D.Q., "Process Heat Transfer", McGraw-Hill Co., New York (1950).

39. Bras, G.H., Chem. Engng. 60 (4), (5), (1953).

40. Cairns, R.C., Chem. Engng. Sci., 3, (1954).

41. Sparrow, E.M., and Lin, S.H., J. Heat and Mass Transfer, Series C, 86, 3, (1964).

42. Rose, J.W., "Condensation of a Vapour in the Presence of a Non-

REFERENCES (CONT.)

Condensing Gas, M.I.T. (Dec. 1967).

43. Rohsenow, W.M., and Choi, H.Y., "Heat, Mass and Momentum Transfer", Prentice-Hall, Inc., (1961).

44. Flügge, W.,"Handbook of Engineering Mechanics", New York, McGraw-Hill, 1962.

45. Langmuir, I., Phys. Rev., 8, 149-176, (1916).

46. Fowler, R.H., "Statistical Mechanics", 2nd Ed., London, Cambridge University Press, (1936).

47. Chapman, S. and Cowling, T.G., "The Mathematical Theory of Non-Uniform Gases", London, Cambridge University Press, (1939).

48. Kaminsky, M., Atomic and Ionic Impact Phenomena on Metal Surface Monograph, (1964).

49. LeFebvre, (M.I.T.) non published.

50. ASME Handbook, New York, McGraw-Hill,(1965).

51. Lemon, A.W., Deem, H.W., Hall, E.H., and Walling, J.P., "The Thermodynamic and Transport Properties of Potassium", Battelle Memorial Institute.

52. Wetherford, W.D., Tyler, J.C., and Ku, P.M., "Properties of Inorganic Energy Conversion and Heat Transfer Fluids for Space Applications", Wadd Technical Report 61-96, (1961).

53. Stephomov, B.I., Timrof, D.L., and Totzki, E.E., Teplophysica vysokich temperatur, Vol. 4, No. 1, (1966).

54. Hirschfelder, J.O. and Curtiss, C.F., "Molecular Theory of Gases and Liquids", John Wiley & Sons, Inc., New York (1954).

55. Subbotin, V.I., Bakolin, N.V., Ivanoskii, M.N., and Sorokin, V.P., Teplofizika vysokich temperatur, Vol. , No. 5, (1967).

56. Frehafer, M.K., Phys. Rev., 15, (1920), 110.

57. Mott, N.F. and Jones, H., "The Theory of the Properties of Metals and Alloys", Oxford University Press, (1936).

58. Probstein, R.F., "Theory and Fundamental Research in Heat Transfer", J. Clark, Pergamon Press, New York, (1963).

APPENDIX A

DIFFERENTIAL EQUATION GOVERNING THE FLOW OF THE CONDENSATE

In his "order of magnitude" analysis, Chapman (11) shows that it is possible to neglect the inertia terms in the momentum equation when

$$\frac{Pr\ h'_{fg}}{C_c \Delta T_w} > 1$$

where Pr is the Prandtl number $= \frac{c\mu}{k}$

h'_{fg} is the heat of vaporization + change of enthalpy corresponding to the average subcooling of a particle

C_c is the specific heat of the liquid condensate

ΔT_w is the temperature drop in the film $= (T_s - T_w)$

Taking as typical values the average temperature of the film equal to 800°F and the temperature drop of 3°F, it comes out for the dimensionless parameter:

$$\frac{Pr\ h_{fg}}{C_c \Delta T_w} = 6.82$$

justifying the aforementioned assumption.

The equation of motion is then simply obtained by balancing the viscous forces and the pressure forces. The scheme of these forces acting on an element (Δx, Δy, 1) is given on Figure 2-b, and the equilibrium can be written:

$$[p - (p + \frac{\partial p}{\partial x} \Delta x)] \Delta y \cdot 1 = [\tau - (\tau - \frac{\partial \tau}{\partial y} \Delta y)] \Delta x \cdot 1$$

with $$p = \rho g (\delta - y)$$

and $$\tau = \mu \frac{\partial u}{\partial y}$$

After simplifications and rearrangement, the differential equation becomes:

$$\frac{\partial^2 u}{\partial y^2} = \frac{\rho g}{\mu} \frac{d\delta}{dx} \quad (1)$$

APPENDIX B

RESOLUTION OF DIFFERENTIAL EQUATION (5)

The differential equation relating the thickness of the film to the temperature drop $(T_s - T_w)$ is:

$$\delta^3(3\delta'^2 + \delta\delta'') = \frac{3k\mu}{\rho^2 g\, h'_{fg}} (T_s - T_w) \qquad (5)$$

which can be written:

$$\delta \frac{d}{dx}\left[\frac{d\delta^4}{dx}\right] = A$$

with $$A = \frac{12k\mu}{\rho^2 h'_{fg} g} (T_s - T_w).$$

The change of variable $t = \frac{d\delta^4}{dx}$ allows a first integration leading to:

$$\frac{d\delta^4}{dx} = \frac{8}{3} A\delta^3 + \text{constant}$$

Developing and setting the constant equal to B, gives

$$\frac{d\delta}{dx} = -\sqrt{\frac{1}{2\delta^3}\left(\frac{B}{\delta^3} + \frac{A}{3}\right)} \qquad (5')$$

For means of symmetry, the film is horizontal at the center of the plate:

$$x = 0 \qquad \delta = \delta_o \qquad \delta' = \delta_o' = 0$$

The constant B can be expressed in terms of δ_o by writing Equation (5')

at x = 0

$$B = \frac{-A\delta_o^3}{3}$$

Replacing B by its value in (5'), and using the dimensionless variable $z = \frac{\delta}{\delta_o}$ leads to:

$$\frac{dz}{dx} = -\left(\frac{A}{6\delta_o^5}\right)^{1/2} \sqrt{\frac{1-z^3}{z^3}}$$

and the integration between 0 and x gives:

$$\int_1^z \frac{z^3\,dz}{\sqrt{1-z^3}} = -\left(\frac{A}{6\delta_o^5}\right)^{1/2} x \qquad (5'')$$

The integral on the left can be broken in two terms:

$$-\int_1^z \sqrt{1-z^3}\,dz - \frac{F}{3^{1/4}}$$

where

$$\frac{F}{3^{1/4}} = \int_z^1 \frac{dz}{\sqrt{1-z^3}}$$

and an integration by parts gives:

$$-\int_1^z \sqrt{1-z^3}\,dz = -\left(z\sqrt{1-z^3} + \frac{3}{2}\int_1^z \frac{z^3\,dz}{\sqrt{1-z^3}}\right)$$

The left-hand member of Equation (5'') becomes:

$$\int_1^z \frac{z^3\,dz}{\sqrt{1-z^3}} = -\frac{3}{2}\int_1^z \frac{z^3\,dz}{\sqrt{1-z^3}} - z\sqrt{1-z^3} - \frac{F}{3^{1/4}}$$

from where the integral under investigation can be calculated:

$$\int_1^z \frac{z^3 dz}{\sqrt{1-z^3}} = -\frac{2}{5}\left[z\sqrt{1-z^3} + \frac{F}{3^{1/4}} \right]$$

giving for Equation (5")

$$\frac{2}{5}\delta_o^{5/2}\left[z\sqrt{1-z^3} + \frac{F}{3^{1/4}} \right] = x\left(\frac{A}{6}\right)^{1/2} \qquad (6')$$

Using the dimensionless parameters already defined:

$$\zeta = \frac{T_s - T_w}{h'_{fg}\,\mu/k} \qquad \Lambda = \zeta^{1/2}\left(\frac{\lambda}{\delta_o}\right)^{5/2}$$

$$x^* = \frac{x}{L} \qquad \lambda = \left[\frac{\mu^2 L^2}{\rho^2 g}\right]^{1/5}$$

Equation (6') can be written:

$$z\sqrt{1-z^3} + \frac{F}{3^{1/4}} = \frac{5}{2^{1/2}}\, x^* \Lambda \qquad (6)$$

Where F is an elliptic integral of the first kind defined by:

$$F(75^o, y) = \int_o^y \frac{ds}{\sqrt{1-\sin^2 75\, \sin^2 s}}$$

with $\cos y = \dfrac{\sqrt{3}-1+z}{\sqrt{3}+1-z}$, $z < 1$

APPENDIX C

DETERMINATION OF THE RELATION $w = G(T_s - T_w)$

Equation (a-6) represents a function x^*_Λ of z with the parameter Λ:

$$x^*_\Lambda = \frac{5}{\Lambda\sqrt{2}} \left(z\sqrt{1-z^3} + \frac{1}{3^{1/4}} F(z)\right) \qquad \text{(a-6)}$$

This function has been plotted for various values of Λ (Table I), and the corresponding values of z for $x^*_\Lambda = 1$ (z_{e_Λ}) have been determined graphically.

Equation (a-8) gives the thickness δ_{o_Λ} for each value of Λ:

$$\left(\frac{\delta_{o_\Lambda}}{\varphi}\right)^5 = \frac{35/12}{\Lambda^2 \dfrac{1 - z_{c_\Lambda}^3}{z_{c_\Lambda}^4}}$$

and definitions (d-3) and (d-4) lead to $(T_s - T_w)_\Lambda$ by :

$$(T_s - T_w)_\Lambda = \frac{\Lambda^2 \mu h'_{fg}}{k} \left(\frac{\delta_{o_\Lambda}}{\varphi}\right)^5$$

Now using the relation (a-7) at the plate's edge:

$$\delta_c = \frac{54}{35} \left(\frac{W_c^2}{\rho^2 g}\right)^{1/3} \qquad \text{(a-7)}$$

the mass flow rate of condensation per unit surface is given by:

$$w = \frac{W_c}{L} = \left(\frac{35}{54} \frac{\delta_c^3 \rho^2 g}{L^2}\right)^{1/2}$$

The values of z_c, δ_o, δ_c, ξ, w, (T_s-T_w) are tabulated in Table 2 for various values of Λ. On Figure 4, w is plotted versus (T_s-T_w).

APPENDIX D

SAMPLE CALCULATION FOR σ

In this section, a sample calculation will be given corresponding to the test No. 1. The parameters obtained experimentally are:

$$T_v = 825.4^oF$$

$$T_w = 809.6^oF$$

$$q_c = 90{,}500 \text{ Btu/hr.ft}^2$$

1-Determination of T_s

To determine T_s, w must be known:

$$w = \frac{q_c}{h_{fg}} = \frac{90{,}500}{907} = 99.7 \text{ lb/hr ft}^2$$

Then, from Figure 4, the theoretical value of (T_s-T_w) is read:

$$(T_s-T_w)_{th} = 3.23^oF$$

This value is to be multiplied by the geometry correction factor, f = 0.8, to obtain the actual value of T_s-T_w.

Then, $T_s = 812.2^oF$

2-Determination of T_i

T_i is determined from Equation (b-4)

$$T_i = \frac{T_v + ST_s}{S+1}$$

with $$S = \frac{k_v}{w\, C_p(\zeta+d)} \quad \text{where } d = 1\lambda \text{ (for this example)}$$

and where ζ and λ can be read on Figure 5. Plot of C_p and k_v are available in References (51) and (53) respectively.

Therefore, $$S = \frac{(0.981)^{10-3}}{(99.7)(0.174)(124+69)^{10-6}} = 2.93$$

and $$T_i = \frac{825.4 + (2.93)(812.2)}{3.93} = 815.56^{o}F$$

The values of the properties λ, k_v and C_p have been taken at temperature T_v. Actually, these quantities should be evaluated at T_i, but for the present experiments the difference is negligible.

However, in the data presented by Sukhatme and Barry an iteration proves to be necessary to obtain an accurate value of T_i.

3-Determination of σ

σ is determined by Equation (c-2):

$$\sigma = \frac{2w}{2y+w}$$

where

$$y = \sqrt{\frac{M}{2\pi RT_i}}\ (p_i - p_s)$$

knowing T_i and T_s, p_i and p_s are calculated from Equation 4.1.

Therefore,

$$y = \sqrt{\frac{39.1}{2(3.14)(1545.3)(1275.3)}}\,(1.036)\sqrt{32.2}(3600)$$

$$= 37.5$$

and finally $$\sigma = \frac{2(99.7)}{2(37.5)+99.7} = 1.14$$

APPENDIX E

DETERMINATION OF THE RADIATIVE HEAT FLUX

As shown in Figure 18, the present system consists of a square horizontal surface (A_1) at temperature T_1. On three sides, (A_1) is surrounded by vertical walls (A_3) 1.5 inches high, at temperature T_3. The fourth side of (A_1) is in contact with an infinite vertical wall of temperature T_2 that is part of the surface (A_2) in which (A_1) and (A_3) are enclosed.

We have therefore the relations between the radiative areas:

$$A_3 = 1.5\ A_1$$

$$A_2 = 1.5\ A_1$$

Diagrams, giving the view factor F for direct radiation between adjacent rectangles in perpendicular planes, are presented in reference (43). F_{1-3} is then found to be:

$$F_{1-3} = 3 \times 0.14 = 0.42$$

then

$$F_{1-2} = 0.58$$

and

$$F_{2-1} = \frac{A_1}{A_2}\ F_{12} = 0.82$$

and

$$F_{2-3} = 0.13$$

In addition, it was assumed that condensation occurred on both surfaces A_1 and A_3. Therefore, $T_1 = T_3$.

The emissivity of the different materials are:

- Surface (A_2): oxidized stainless steel, $\varepsilon_2 = 1$ (43)

- Surfaces (A_1) and (A_3): liquid potassium at temperature T_1: $\varepsilon_1 = \varepsilon_3 = 0.06 \frac{T\ ^oR}{520}$ (56) (57)

Therefore, the system can be represented by the electrical analog of Figure 18, where

$$R_1 = \frac{1}{A_1 F_{12}}$$

$$R_2 = \frac{1}{A_2 F_{23}}$$

$$R_3 = \frac{1-\varepsilon_1}{A_1 \varepsilon_1}$$

$$R_4 = \frac{1}{A_1 F_{13}}$$

and

$$R_5 = \frac{1-\varepsilon_3}{A_3 \varepsilon_3} \quad R_4$$

It is therefore possible to solve this circuit and the radiative heat flux q_r is given by:

$$\frac{q_r}{A_1} = \frac{1}{15.09}\ \sigma^* \ (T^4 - T_o^4)$$

where σ^* = Stefan-Boltzmann Constant.

z	x^*	x^*	x^*	x^*	x^*	x^*	x^*	x^*
1.0	0	0	0	0	0	0	0	0
0.8	0.938	0.876	0.82	0.774	0.731	0.693	0.671	0.663
0.6	1.26	1.18	1.11	1.04	0.986	0.935	0.907	0.894
0.4				1.14	1.08	1.02	0.993	0.978
0.2					1.10	1.04	1.01	0.998
Λ	0.28	0.30	0.32	0.34	0.36	0.38	0.39	0.395

TABLE 1

DETERMINATION OF $x^*_\Lambda(z)$ FOR DIFFERENT VALUES OF THE PARAMETER Λ

Λ	z_c	δ_o ft x 10^{-3}	δ_c ft x 10^{-3}	w lbm/hr x ft^2	$T_s - T_w$ °F
0.28	0.775	2.69	2.08	585	43
0.30	0.735	2.49	1.83	483	33.2
0.32	0.695	2.25	1.56	380	22.4
0.34	0.640	2.01	1.29	282	14.4
0.36	0.58	1.78	1.03	204	9
0.38	0.48	1.47	0.71	114	3.8
0.39	0.35	1.10	0.39	41.8	0.99

TABLE 2

DETERMINATION OF THE RELATION $w = G(T_s - T_w)$

T_v	T_w	q_c	T_s	p_v	p_s	λ	T_i deg.F			σ		
deg.F	deg.F	Btu/hr, ft^2	deg.F	atm.	atm.	ftx10^{-6}	d=1λ	d=3λ	d=10λ	1λ	3λ	10λ
825.4	809.6	90500	812.2	0.0139	0.0120	67.0	815.56	817.0	819.81	1.14	0.97	0.74
832.8	822.2	71900	823.9	0.0152	0.0137	61.0	825.67	826.83	828.32	1.27	1.03	0.82
846.6	840.1	46300	841.1	0.0173	0.0164	53.0	841.76	842.13	843.10	1.52	1.37	1.02
920.7	912	104600	913.7	0.0363	0.0328	26.3	914.33	914.70	915.70	1.25	1.03	0.69
1047.0	1031	91300	1034.3	0.1017	0.0918	9.4	1034.90	1035.29	1036.41	1.28	1.03	0.67
1056.9	1045	79600	1046.8	0.1081	0.1019	8.5	1047.08	1047.26	1047.83	1.55	1.35	0.96
1062.1	1056	116600	1057.5	0.1148	0.1100	7.9	1057.61	1057.69	1057.92	1.61	1.41	1.04
1087.2	1075	98200	1077.9	0.1396	0.1300	7.0	1078.21	1078.41	1079.04	1.41	1.19	0.79
1110.0	1093	69000	1094.8	0.1665	0.1496	6.4	1095.13	1095.34	1096.04	1.21	0.96	0.58
1126.4	1106	69400	1109.8	0.1895	0.1720	5.8	1110.36	1110.70	1111.80	1.24	1.00	0.62
1193.5	1181	64300	1182.6	0.2983	0.2770	3.9	1182.73	1182.82	1183.15	1.36	1.11	0.67
1290.0	1269	119700	1273.1	0.5662	0.4970	2.2	1273.32	1273.45	1273.91	1.08	0.85	0.49

TABLE 3

EXPERIMENTAL DATA AND RESULTS FOR SATURATED POTASSIUM VAPOR CONDENSING ON A HORIZONTAL SURFACE

T_v	T_w	q_c	T_s	p_v	p_s	λ	T_i deg.F			σ		
deg.F	deg.F	Btu/hr. ft^2	deg.F	atm.	atm.	ftx10^{-6}	1 λ	3 λ	10 λ	1 λ	3 λ	10 λ
805.50	799.00	44078	799.44	0.0106	0.0099	74.5	800.38	800.88	802.06	1.48	1.31	1.02
811.00	800.00	80968	800.99	0.0112	0.0100	71.0			806.71			0.915
850.73	843.50	45864	843.97	0.0172	0.0160	48.5	844.71	845.13	846.24	1.43	1.24	0.906
914.00	902.00	80926	903.20	0.0324	0.0291	26.5	904.32	904.97	906.69	1.28	1.06	0.73
1017.30	1012.00	41355	1012.42	0.0807	0.0775	11.0	1012.53	1012.60	1012.84	1.64	1.47	1.10
1052.50	1049.83	34403	1050.16	0.1070	0.1051	8.2	1050.19			1.84		
1055.00	1050.20	53970	1050.81	0.1092	0.1056	8.1	1050.90	1050.96	1051.15	1.70	1.54	1.20
1132.75	1129.91	36023	1130.27	0.1947	0.1913	5.3	1130.29	1130.31	1130.36	1.83	1.69	1.41
1233.50	1227.39	45571	1227.90	0.3807	0.3675	3.0	1227.93	1227.96	1228.04	1.70	1.47	1.09
1305.00	1295.00	98824	1296.48	0.5849	0.5567	1.8	1296.56	1296.60	1296.73	1.52	1.36	1.00

TABLE 4

σ CALCULATED FROM KROGER'S DATA FOR POTASSIUM

T_v	T_w	q_c	T_s	p_v	p_s	λ	T_i deg.F			σ		
deg.F	deg.F	Btu/hrft^2	deg.F	atm.	atm.	ftx10^{-6}	1λ	3λ	10λ	1λ	3λ	10λ
1240	1211	290000	1213	0.100	0.082	39.7	1219.96	1223.46	1229.67	0.69	0.52	0.36
1263	1234	286000	1236	0.120	0.096	34.3	1241.69	1245.35	1251.79	0.67	0.46	0.31
1280	1252	271000	1254	0.135	0.112	30.0	1258.89	1261.90	1267.95	0.72	0.52	0.33
1299	1270	281000	1272	0.152	0.128	27.0	1276.64	1279.61	1285.80	0.74	0.53	0.33
1341	1315	255000	1317	0.204	0.175	21.2	1320.17	1322.33	1326.36	0.75	0.53	0.34
1370	1346	261000	1348	0.249	0.214	18.2	1350.33	1352.37	1356.66	0.79	0.52	0.30
1396	1367	269000	1369	0.286	0.247	16.4	1371.74	1374.04	1379.56	0.78	0.52	0.28
1416	1383	417000	1386	0.326	0.271	14.9	1390.46	1393.28	1399.51	0.64	0.45	0.27
1492	1456	352000	1459	0.507	0.429	10.1	1461.91	1464.02	1469.54	0.65	0.44	0.24
1508	1481	297000	1483	0.558	0.488	9.1	1484.72	1486.09	1489.83	0.75	0.50	0.26
1525	1479	519000	1484	0.610	0.491	8.6	1488.68	1491.30	1499.07	0.91	0.59	0.22

TABLE 5

σ CALCULATED FROM BARRY'S DATA FOR SODIUM

T_v	T_w	q_c	T_s	p_v	p_s	λ	T_i deg.F			σ		
deg.F	deg.F	Btu/hr.ft^2	deg.F	atm.	atm.	ft x 10^{-6}	1 λ	3 λ	10 λ	1 λ	3 λ	10 λ
434	423.7	46800	424	0.047	0.040	19.7	425.13	425.82	427.56	1.35	1.06	0.73
436	425	55400	426	0.048	0.041	19.0	427.27	428.03	429.86	1.31	1.09	0.77
439	426	73200	427	0.051	0.042	18.8	428.65	429.60	431.88	1.29	1.07	0.79
441	426.4	104800	428	0.503	0.043	18.5	430.73	432.11	434.95	1.19	0.98	0.73
674	663	124000	665	0.994	0.926	1.7	665.20	665.30	665.80	1.42	1.18	0.75

TABLE 6

σ CALCULATED FROM MISRA'S DATA FOR MERCURY

T_v	T_w	q_c	T_s	p_v	p_s	λ	T_i deg.F			σ		
deg.F	deg.F	Btu/hr ft^2	deg.F	atm.	atm.	ft x 10^{-6}	1λ	3λ	10λ	1λ	3λ	10λ
342	329	47600	330	0.009	0.00707	64.0	333.72	335.21	338.00	1.38	1.19	1.03
369	351.5	73150	353	0.015	0.0113	45.0	358.31	360.41	363.91	1.23	1.12	0.88
381	366.5	72500	368	0.019	0.0150	39.0	371.83	373.47	376.38	1.31	1.15	0.94

TABLE 7

σ CALCULATED FROM SUKHATME'S DATA FOR MERCURY

Test	T_i	T_o	W	t	$q_{c\ th}$	$q_{c\ exp}$	q_r	$h_{c\ th}$	$h_{c\ exp}$	$\frac{h_{exp}-h_{th}}{h_{th}}$
No.	deg.F	deg.F	$lbm \times 10^{-6}$	inches	$Btu/hr.ft^2$	$Btu/hr.ft^2$	$Btu/hr.ft^2$	$Btu/hr.ft^2 {}^\circ F$	$Btu/hr.ft^2 {}^\circ F$	%
1	1180	655	0.33	0.0049	65800	61100	648	125.3	115.1	8.16
2	1195	575	0.83	0.0107	30400	33500	728	49.1	52.8	7.56
3	1230	620	0.6	0.0064	51450	59500	777	84.3	91.4	8.45
4	1185	418	1.97	0.0261	12650	11566	766	16.5	14.1	14.5

TABLE 8

EXPERIMENTAL DATA AND RESULTS FOR POTASSIUM CONDENSING IN THE PRESENCE OF HELIUM

Test	T_i	T_o	W	t	$q_{c\ th}$	$q_{c\ exp}$	q_r	$h_{c\ exp}$	$h_{c\ th}$	$\frac{h_{exp}-h_{th}}{h_{th}}$
No.	^oF	^oF	$lbm 10^{-5} in.$	$10^{-3} in.$	$Btu/hr.ft^2$	$Btu/hr.ft^2$	$Btu/hr.ft^2$	$Btu/hrft^2{}^oF$	$Btu/hrft^2{}^oF$	-
1	1175	411	9.25	9.65	9250	14000	764	18.3	12.1	0.512
2	1200	489	8.76	6.5	11400	19900	769	28.0	16.0	0.75
3	1057	245	9.95	20.6	3185	6720	568	8.27	3.93	1.10
4	1220	380	9.32	5.9	12500	16080	849	20.0	14.9	0.342
5	1106	285	8.95	13.7	6550	12100	645	14.53	7.9	0.845
6	1001	774	0.64	2.99	26610	27000	229	118	117	0.01
7	1152	636	2.29	3.27	26250	31200	604	59.4	51.9	0.145
8	1092	454	6.21	11.4	7650	12950	671	19.15	12.0	0.596

TABLE 9

EXPERIMENTAL DATA AND RESULTS FOR POTASSIUM CONDENSING IN THE PRESENCE OF ARGON

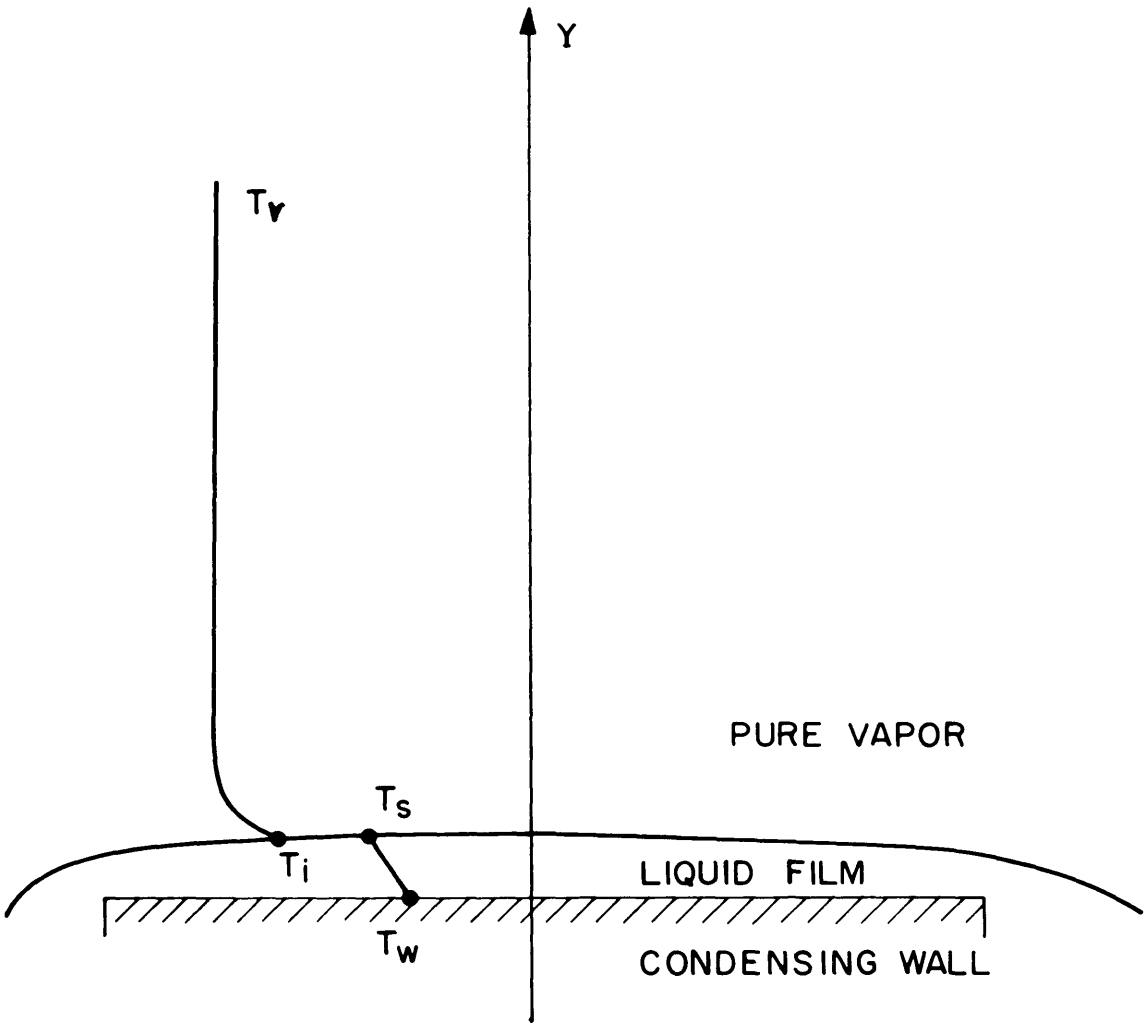

FIGURE I TEMPERATURE DISTRIBUTION IN THE VAPOR AND THE LIQUID DURING THE PROCESS OF CONDENSATION ON A HORIZONTAL PLATE

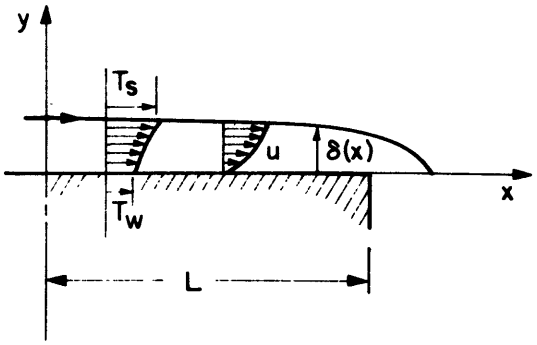

FIGURE 2-a

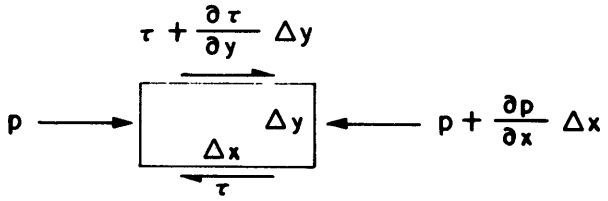

FIGURE 2-b

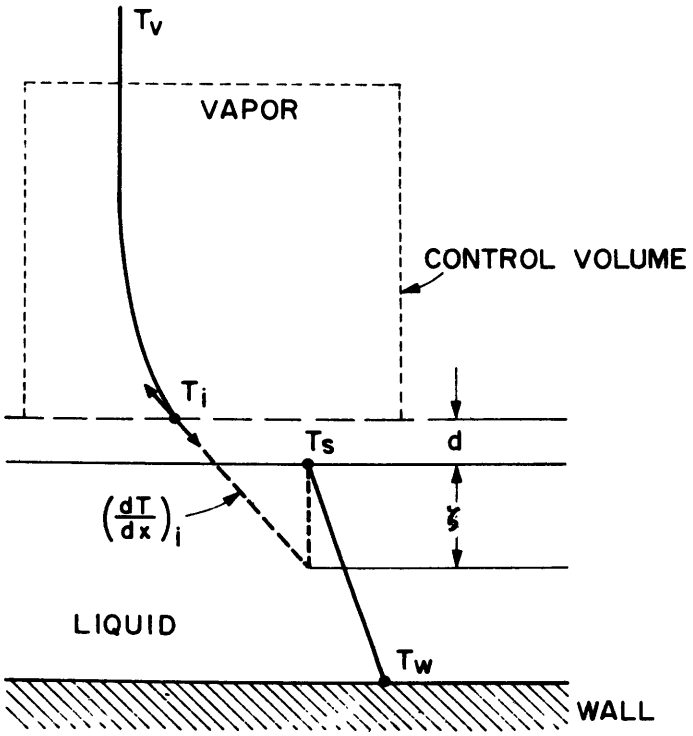

FIGURE 3

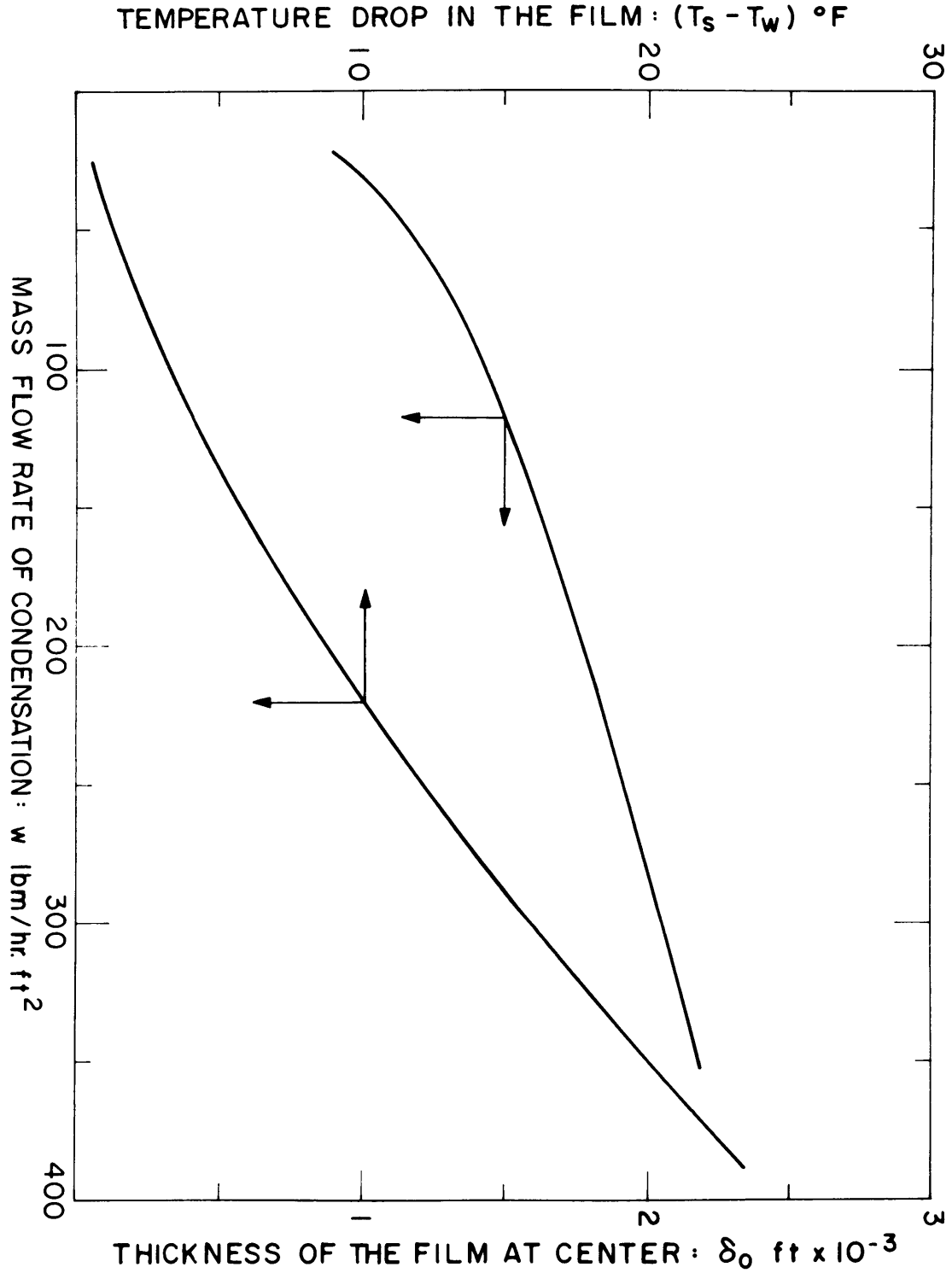
TEMPERATURE DROP IN THE FILM : $(T_s - T_w)$ °F
10
20
30
MASS FLOW RATE OF CONDENSATION : w lbm/hr. ft^2
100
200
300
400
1
2
3
THICKNESS OF THE FILM AT CENTER : δ_o ft x 10^{-3}

FIGURE 4

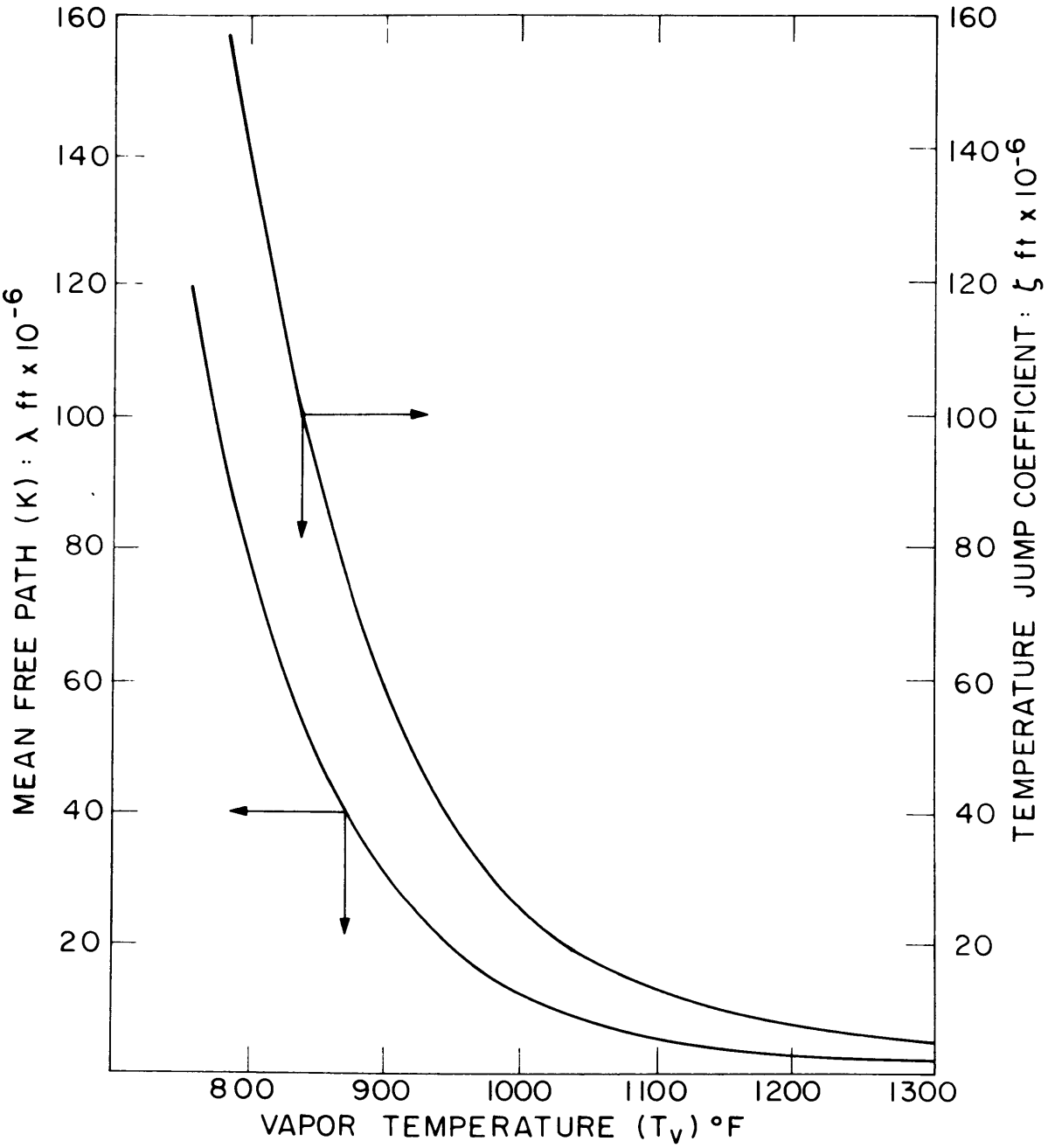
160
140
120
100
80
60
40
20
MEAN FREE PATH (K) : λ ft x 10⁻⁶
TEMPERATURE JUMP COEFFICIENT : ζ ft x 10⁻⁶
800
900
1000
1100
1200
1300
VAPOR TEMPERATURE (Tv) °F

FIGURE 5

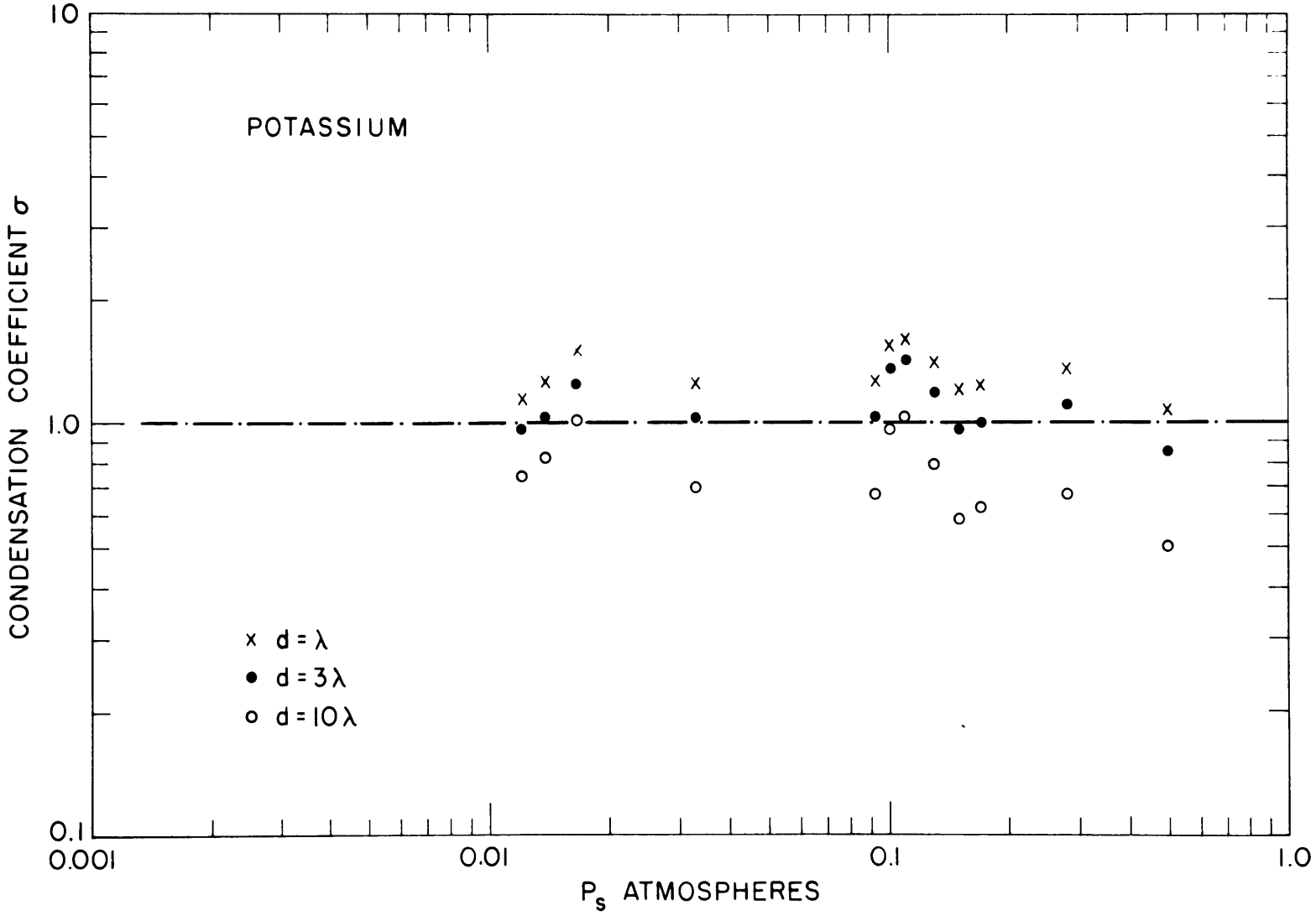

FIGURE 6-a CONDENSATION COEFFICIENT VS. SATURATION PRESSURE

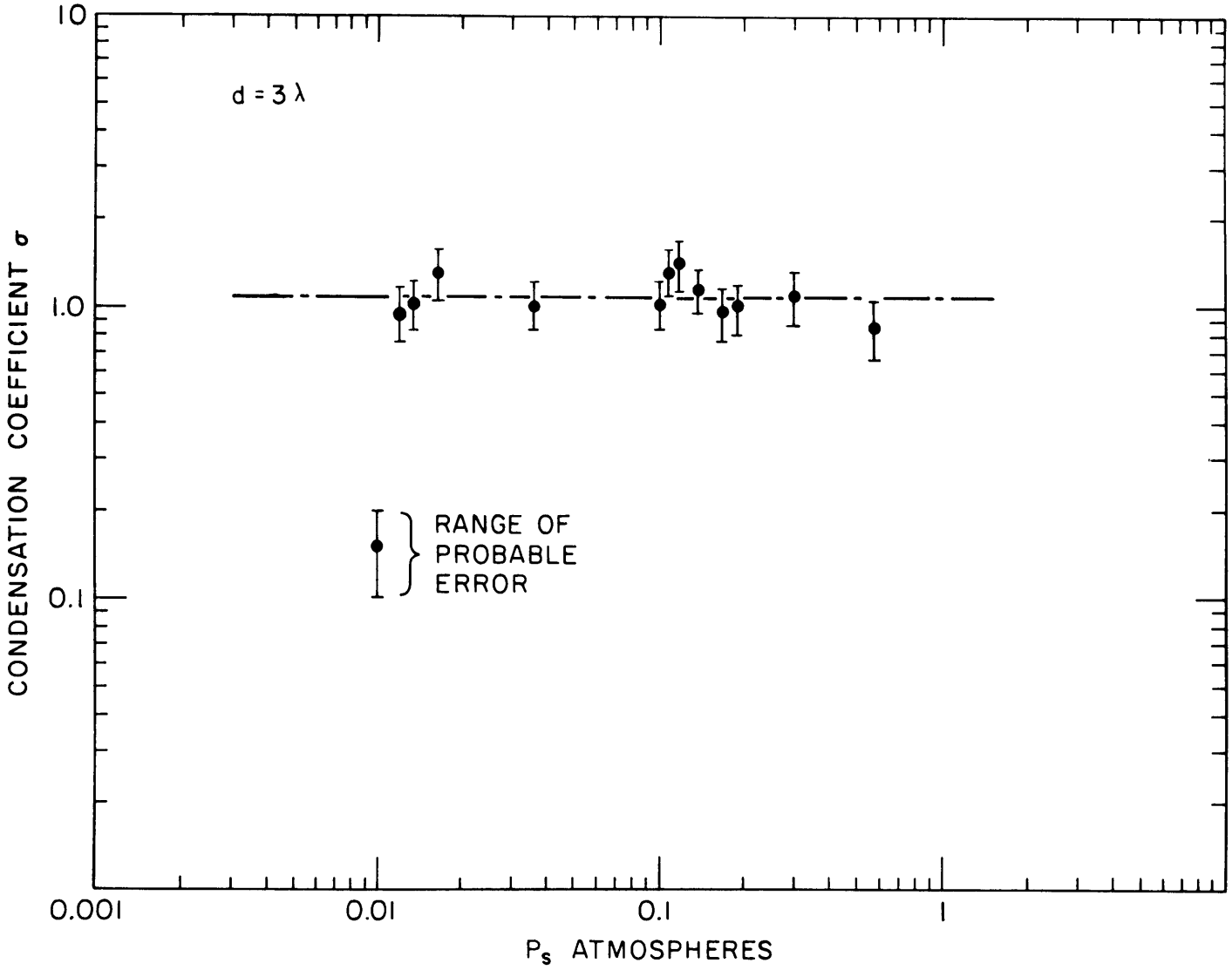

FIGURE 6-b CONDENSATION COEFFICIENT VS. SATURATION PRESSURE

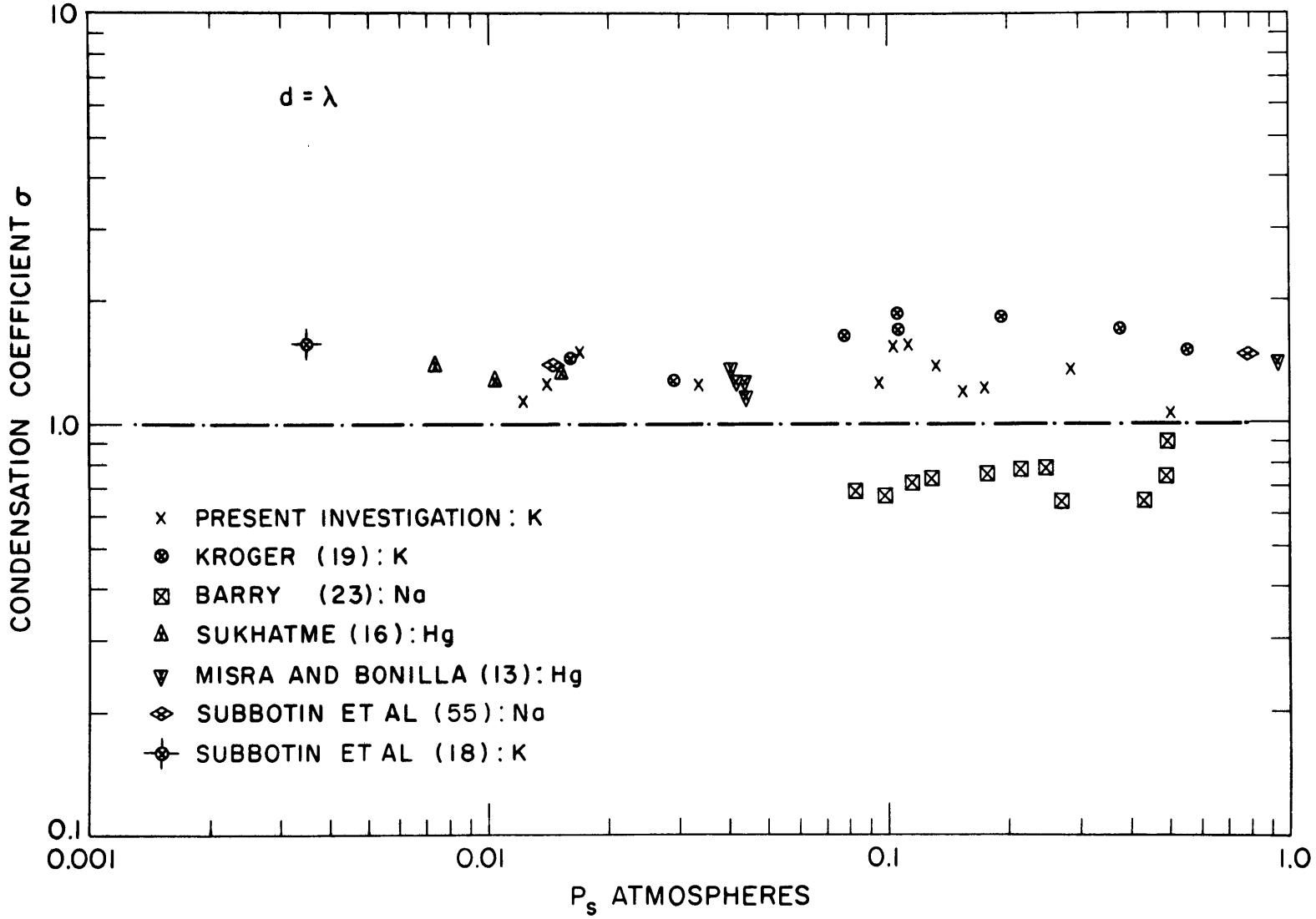

FIGURE 7-a CONDENSATION COEFFICIENT VS. SATURATION PRESSURE

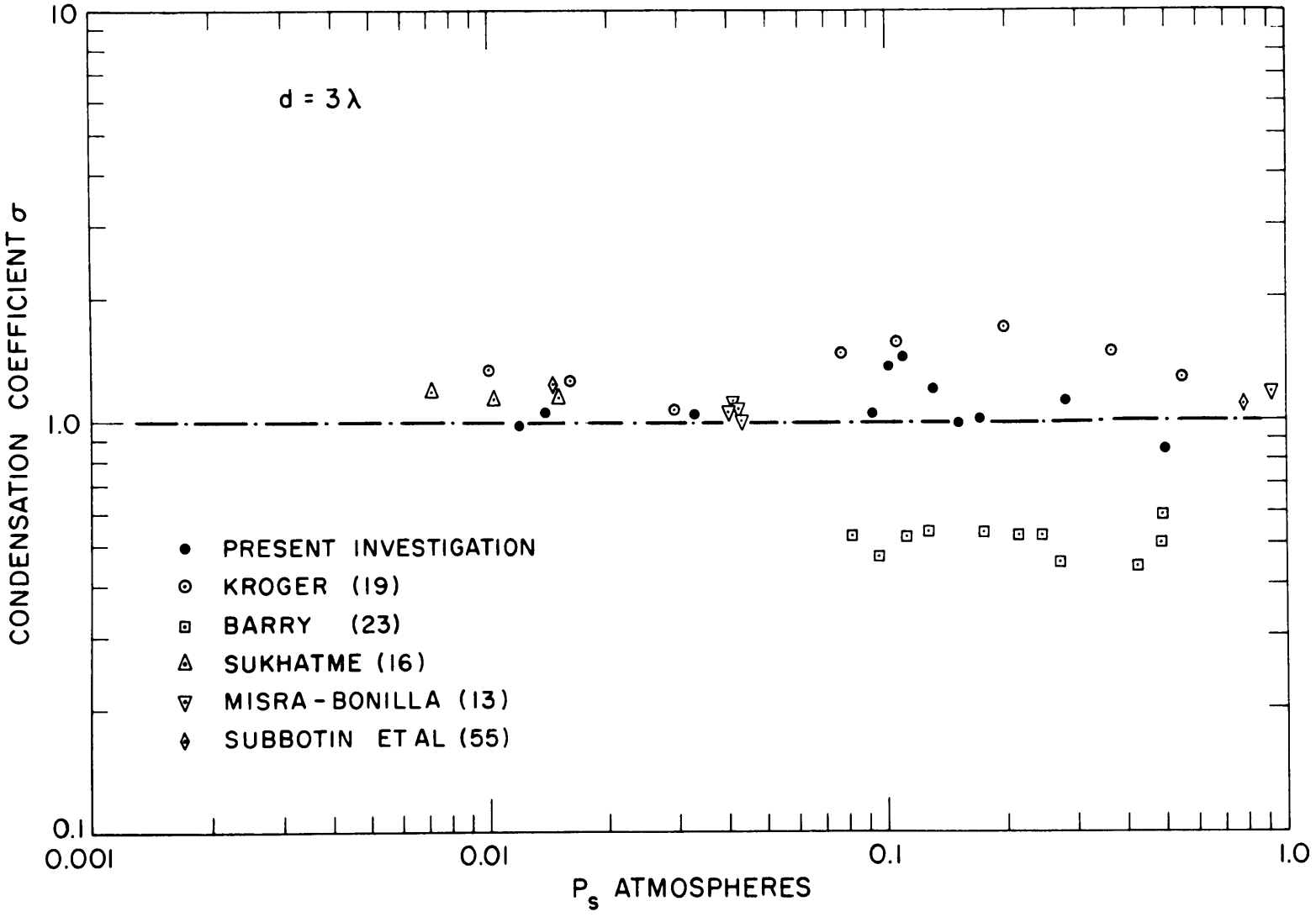

FIGURE 7-b CONDENSATION COEFFICIENT VS. SATURATION PRESSURE

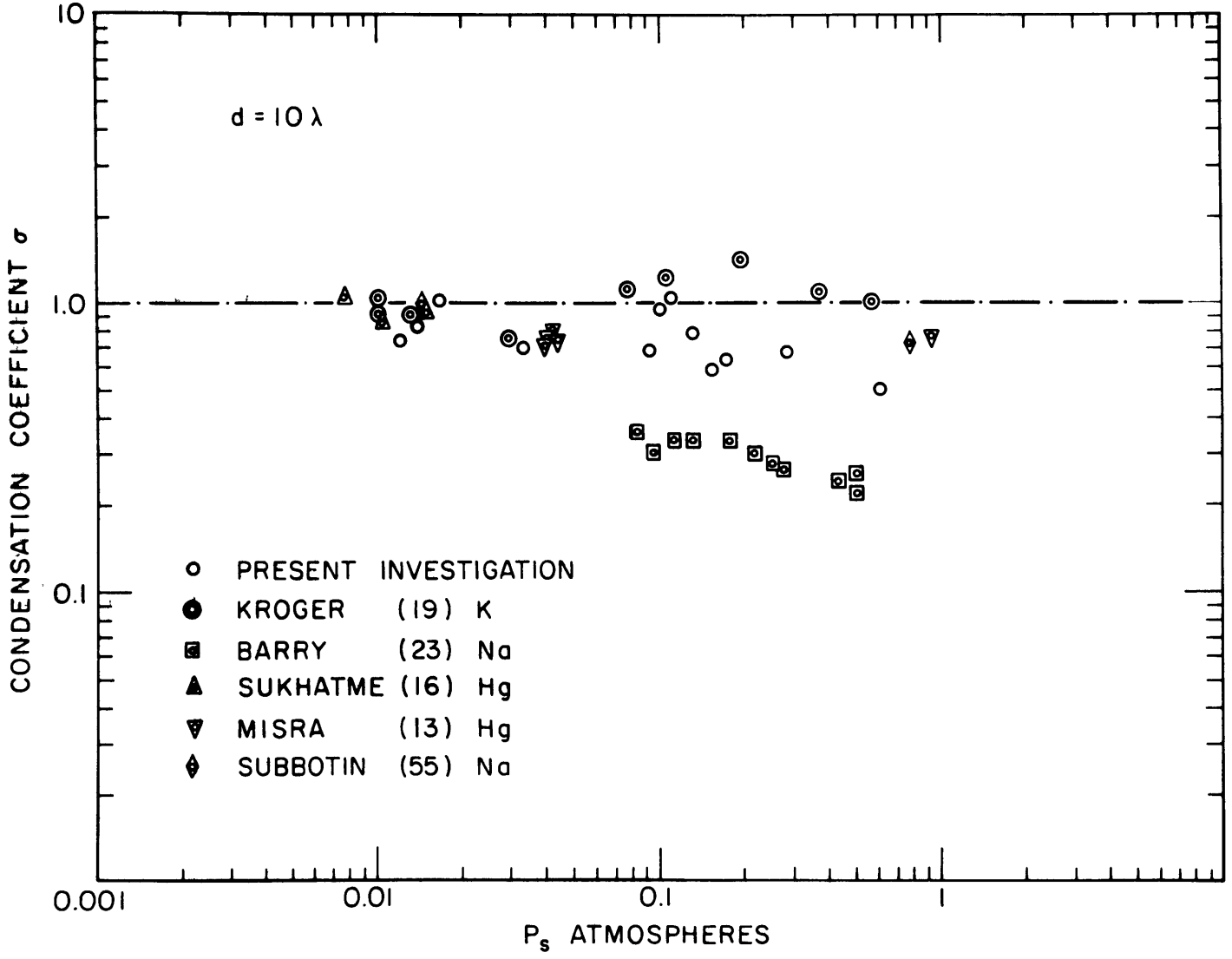

FIGURE 7-c CONDENSATION COEFFICIENT VS. SATURATION PRESSURE

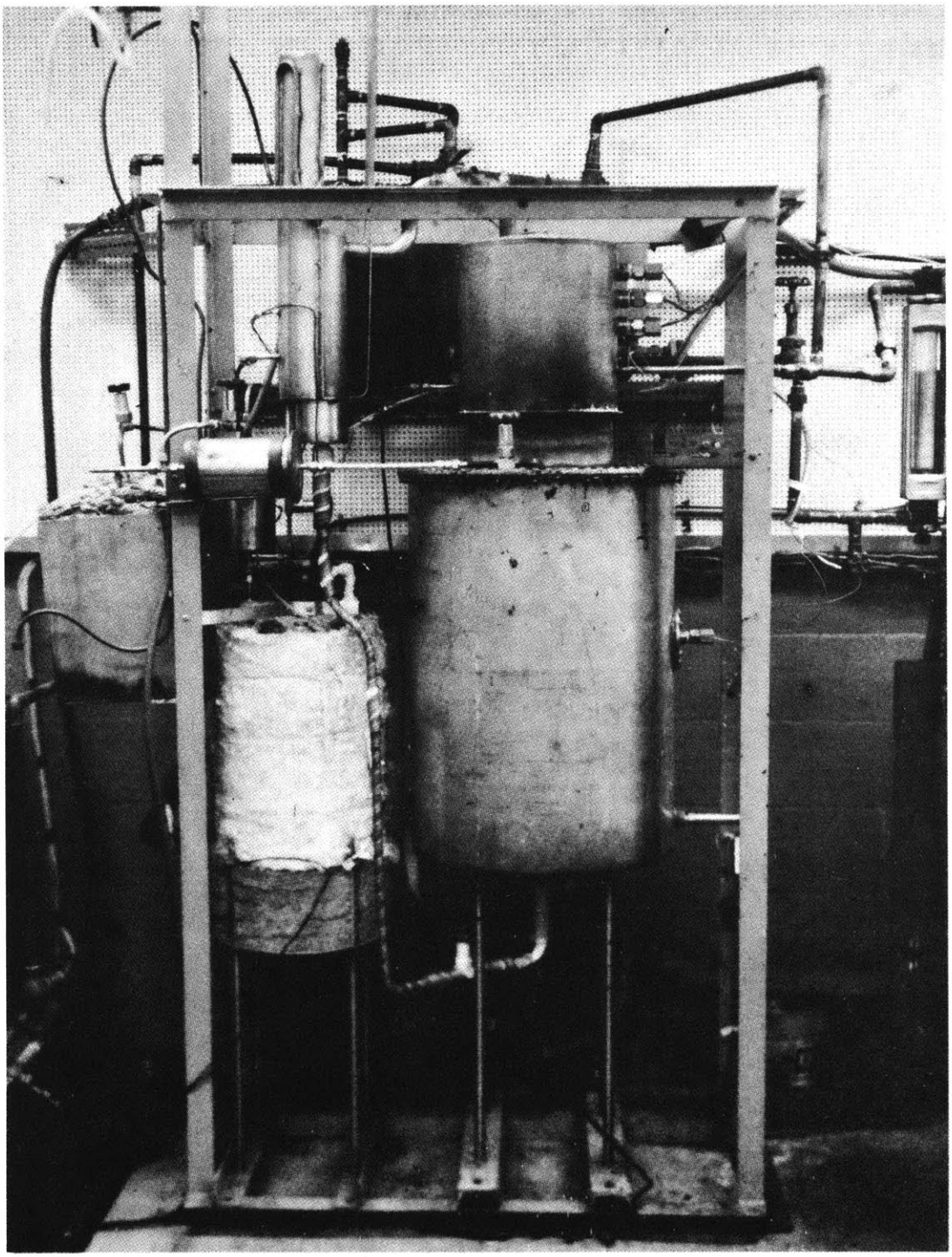

FIGURE 8 APPARATUS

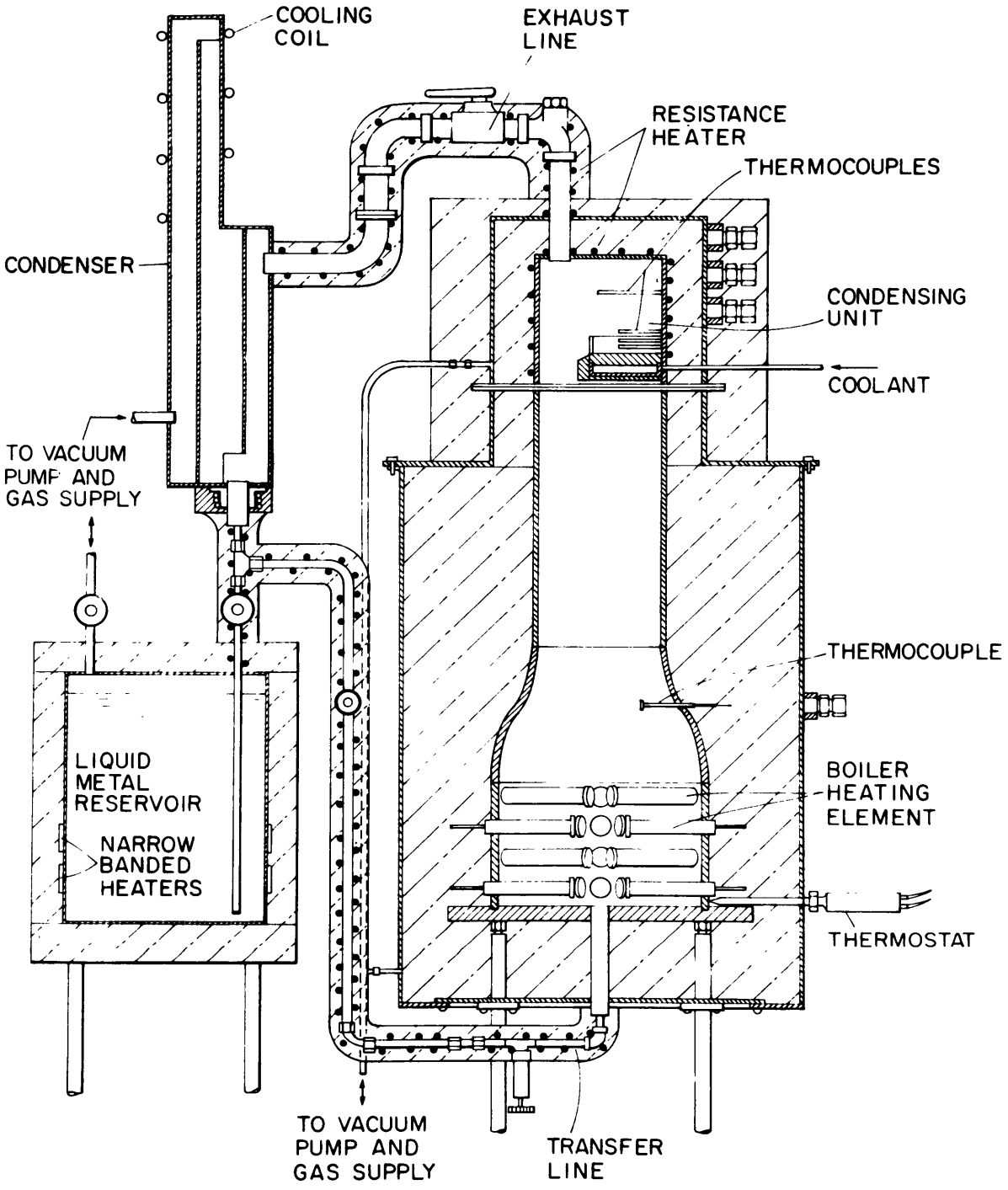

FIGURE 9 APPARATUS

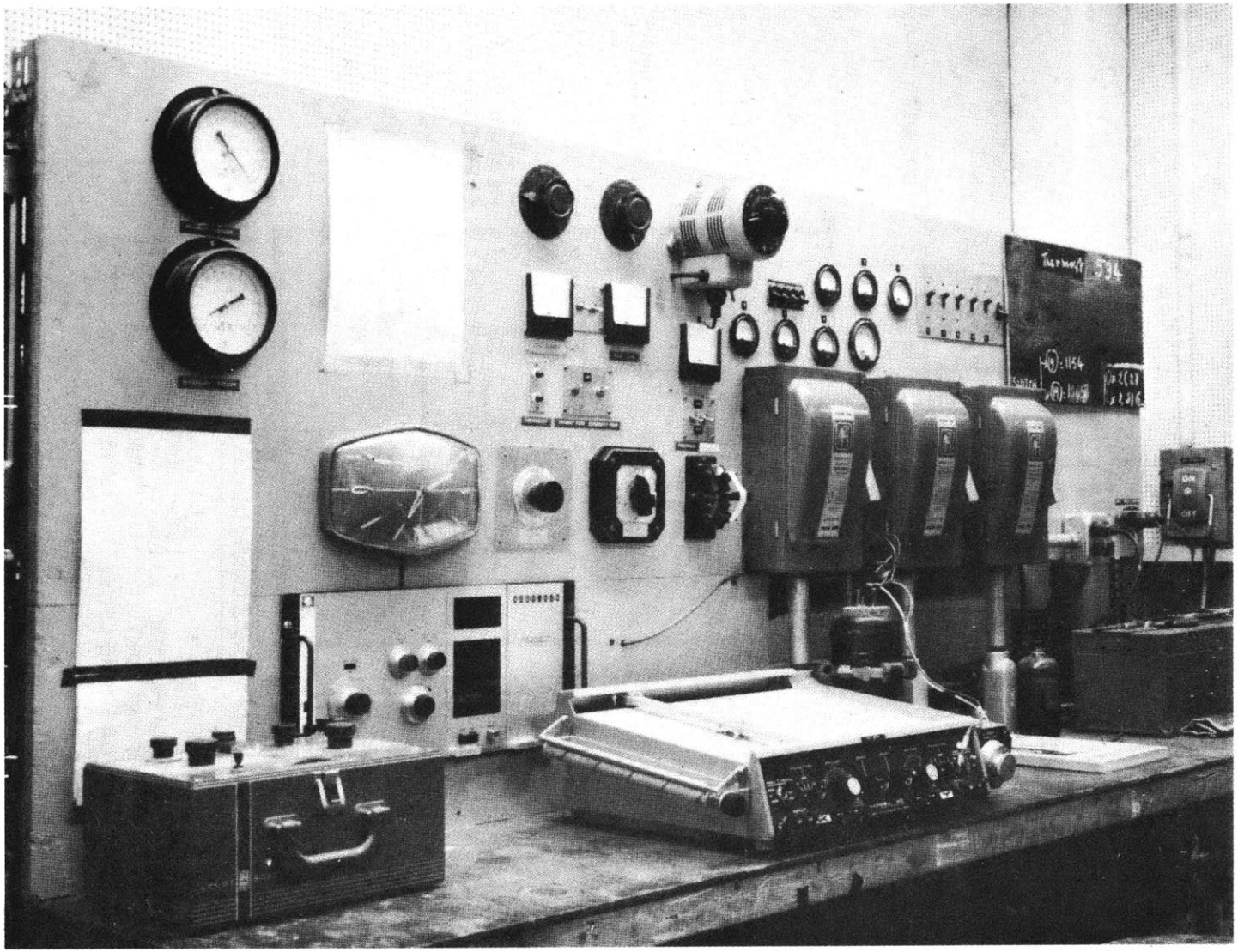

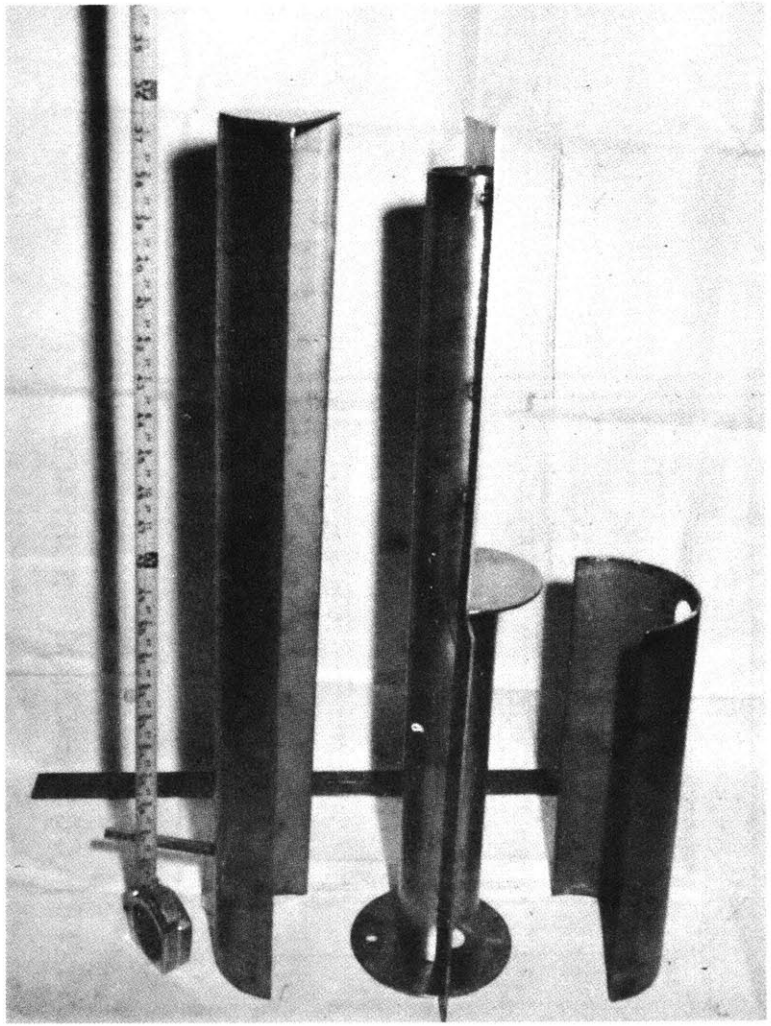

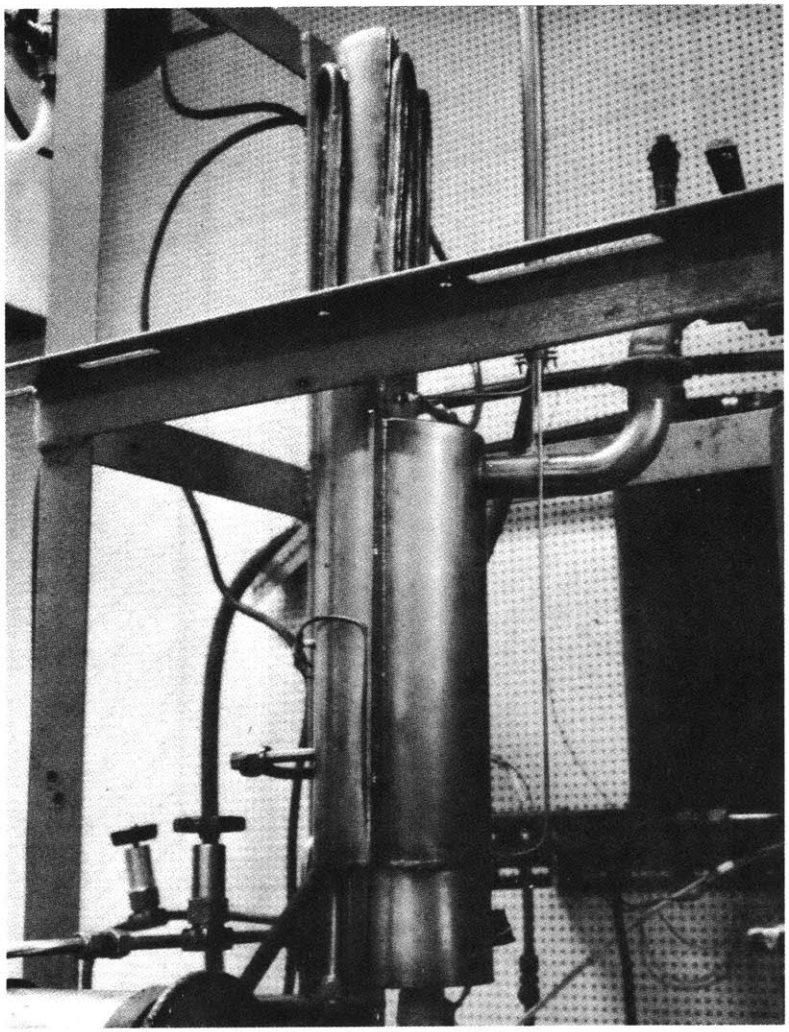

FIGURE 11 CONDENSER

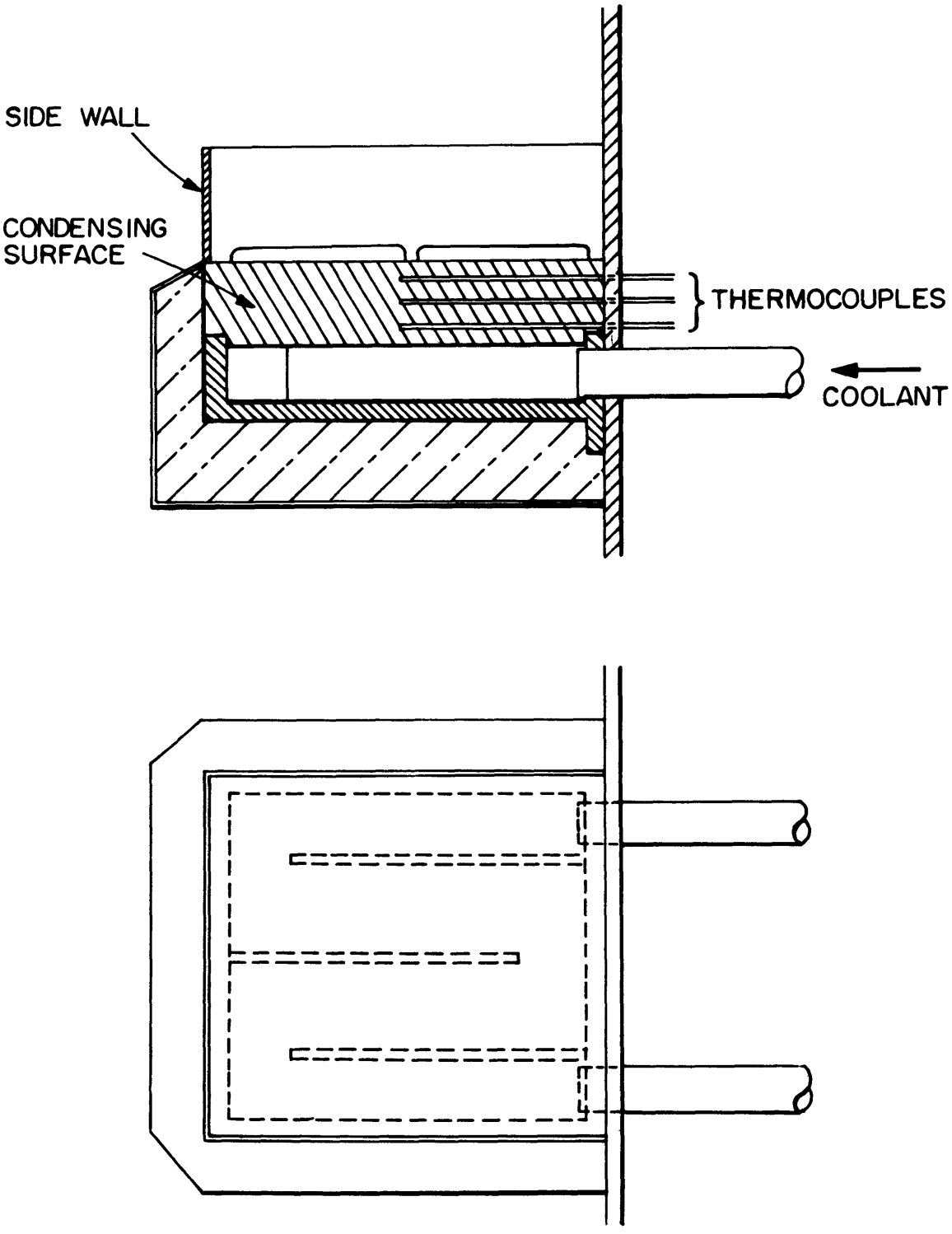

FIGURE 12 CONDENSING SURFACE

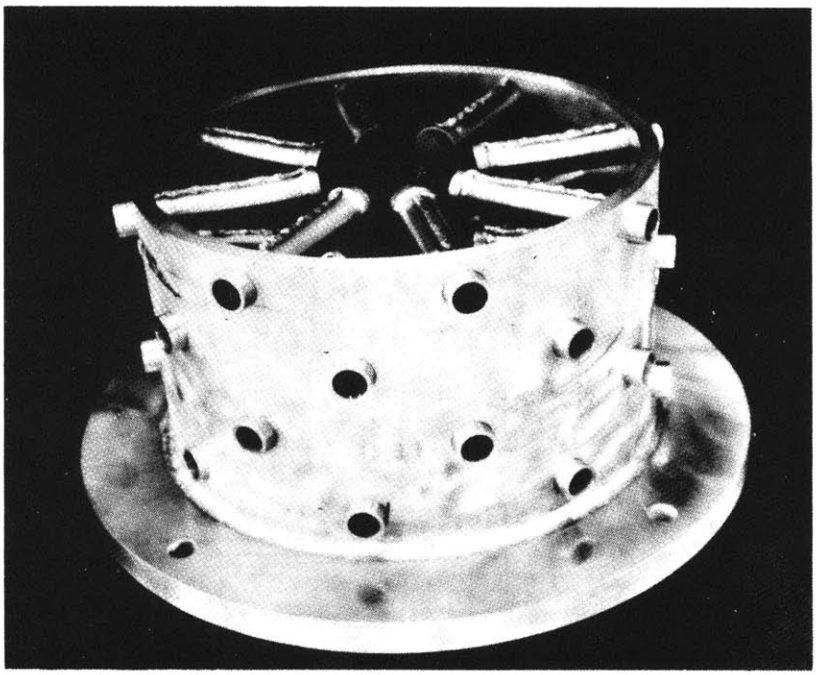

FIGURE 13 BOILER SECTION

FIGURE 14 BOILER, AND JACKET

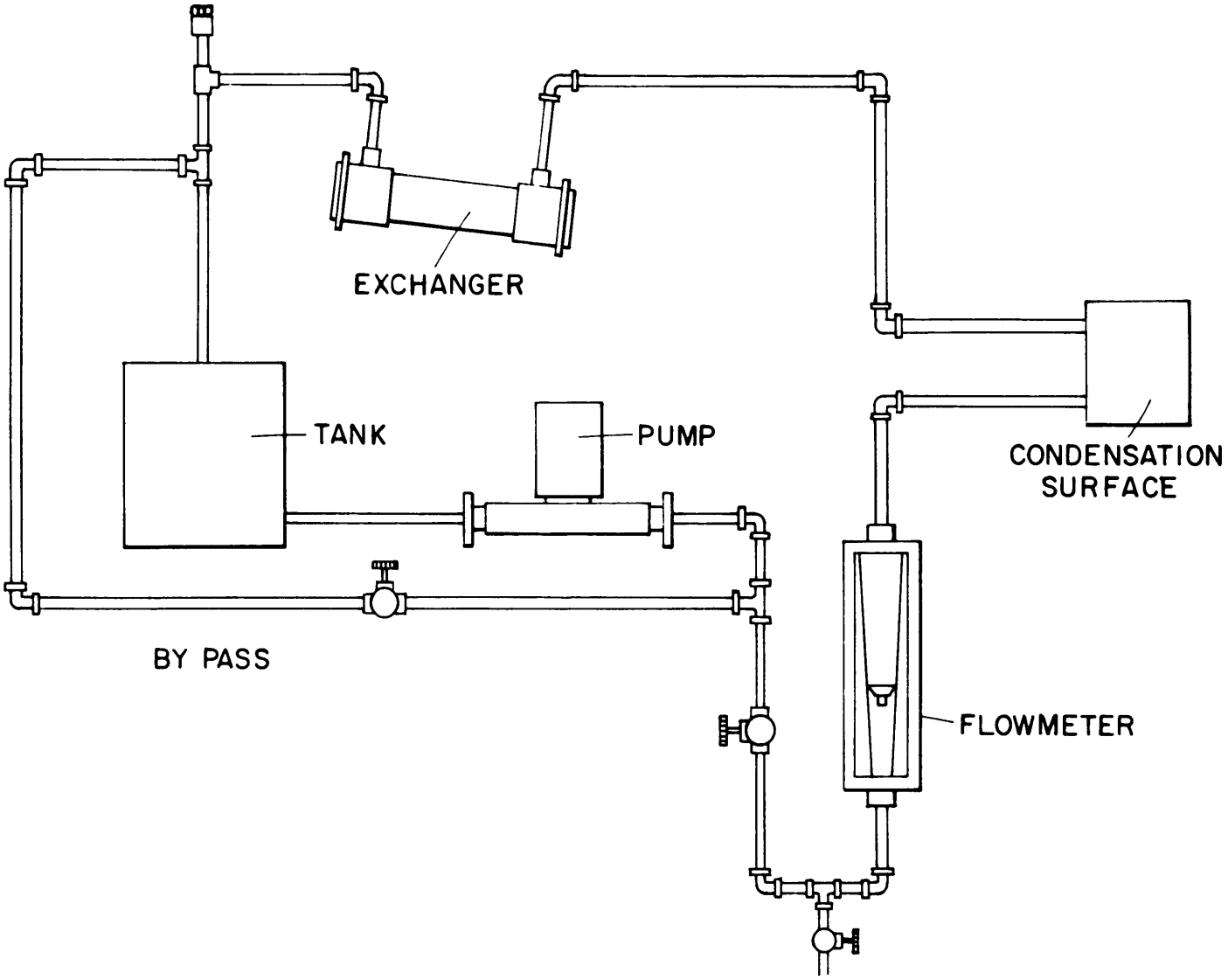

FIGURE 15 COOLING SYSTEM

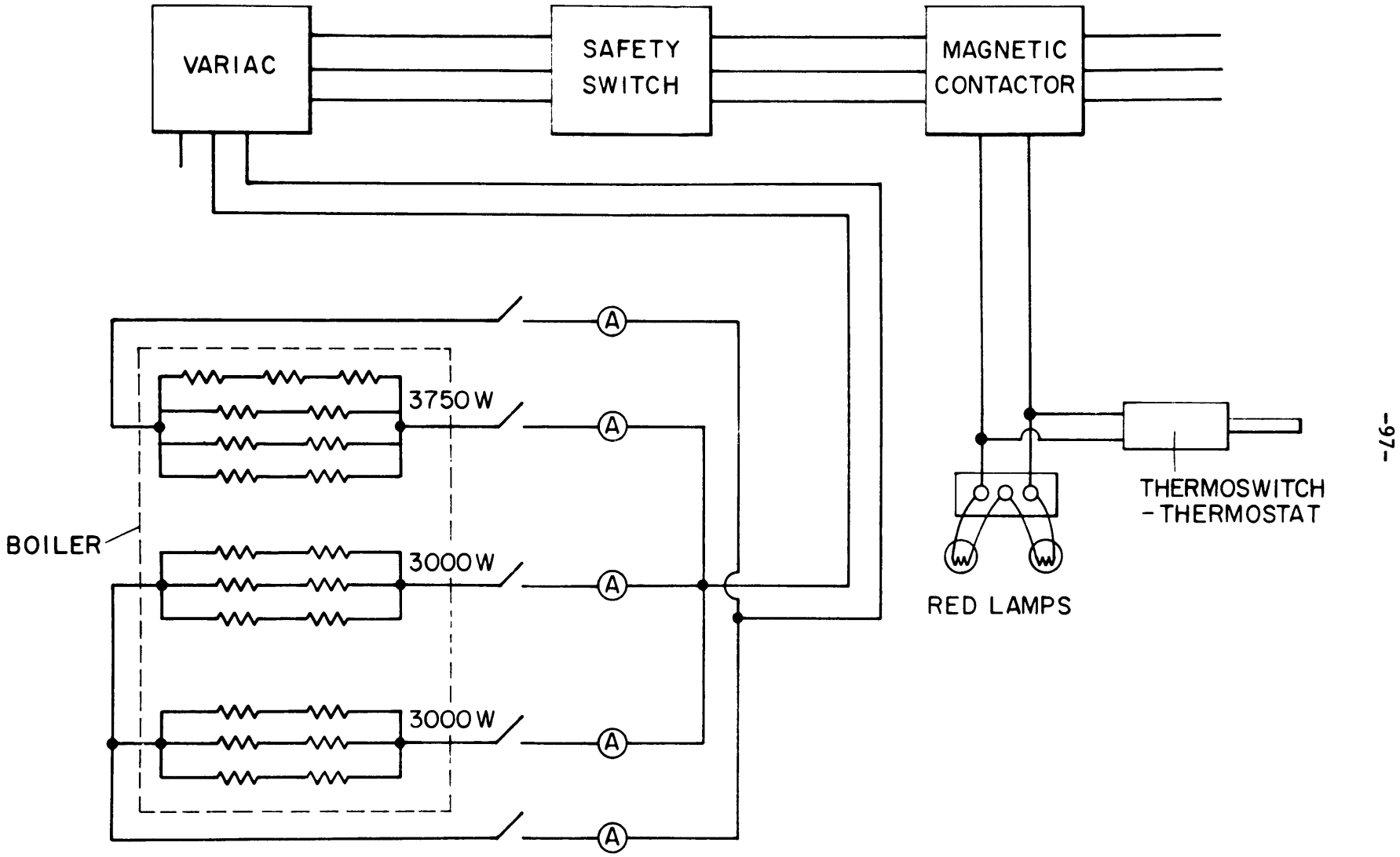

FIGURE 16 ELECTRICAL NETWORK OF THE HEATING SYSTEM

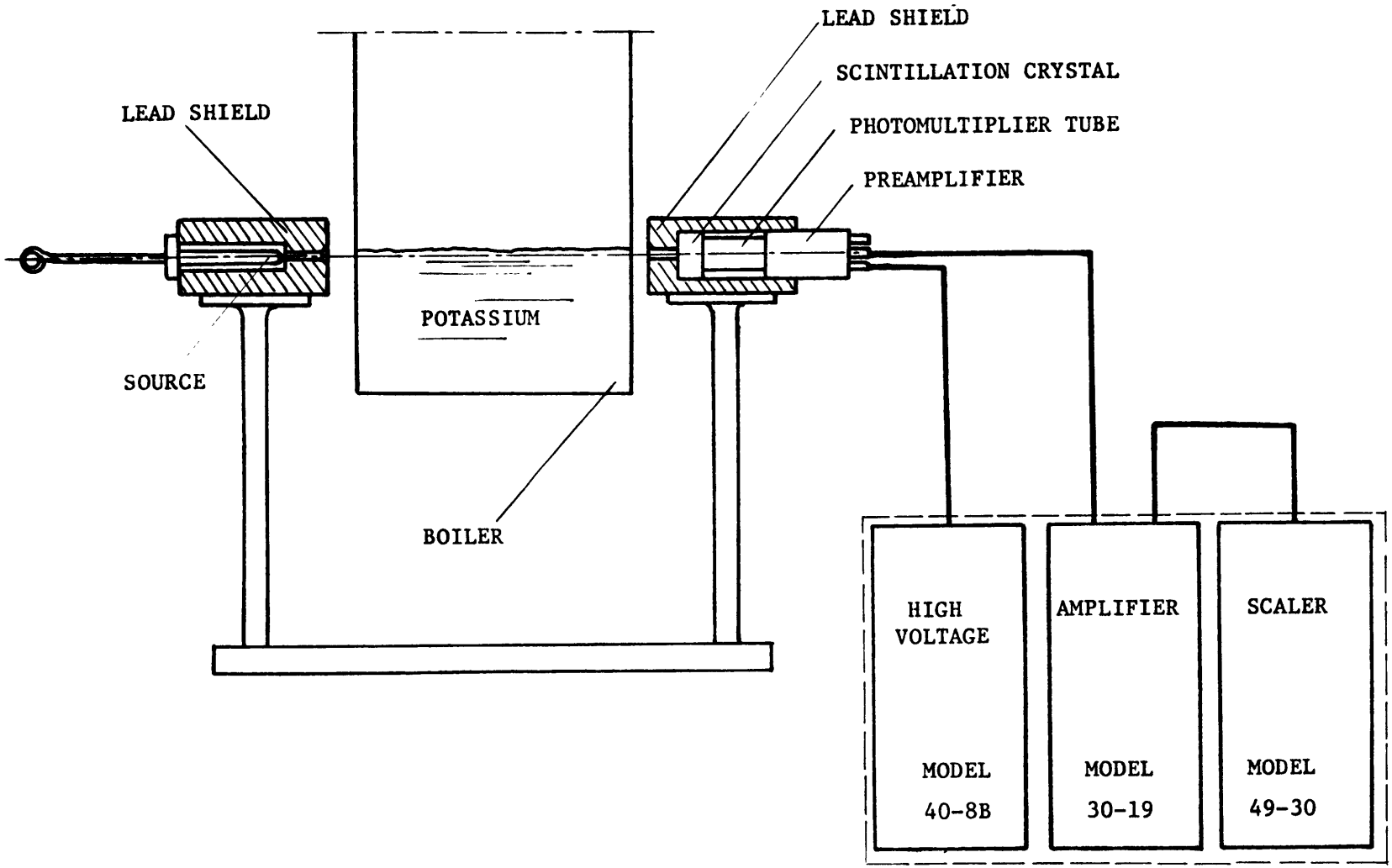

FIGURE 17 DETECTION OF THE LIQUID METAL LEVEL IN THE BOILER

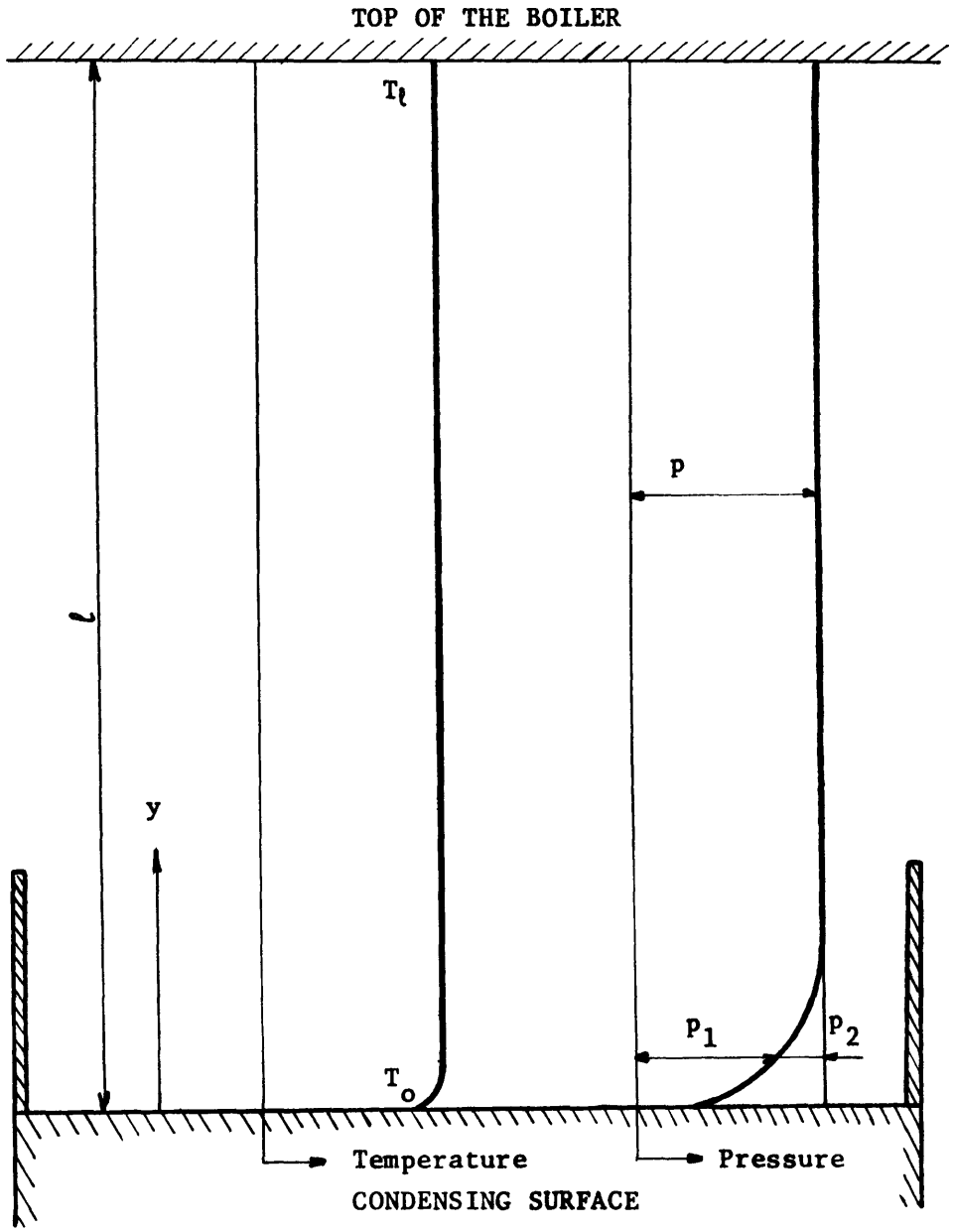

FIGURE 18 TEMPERATURE AND PARTIAL PRESSURE OF THE VAPOR DURING CONDENSATION IN PRESENCE OF A NON-CONDENSABLE GAS

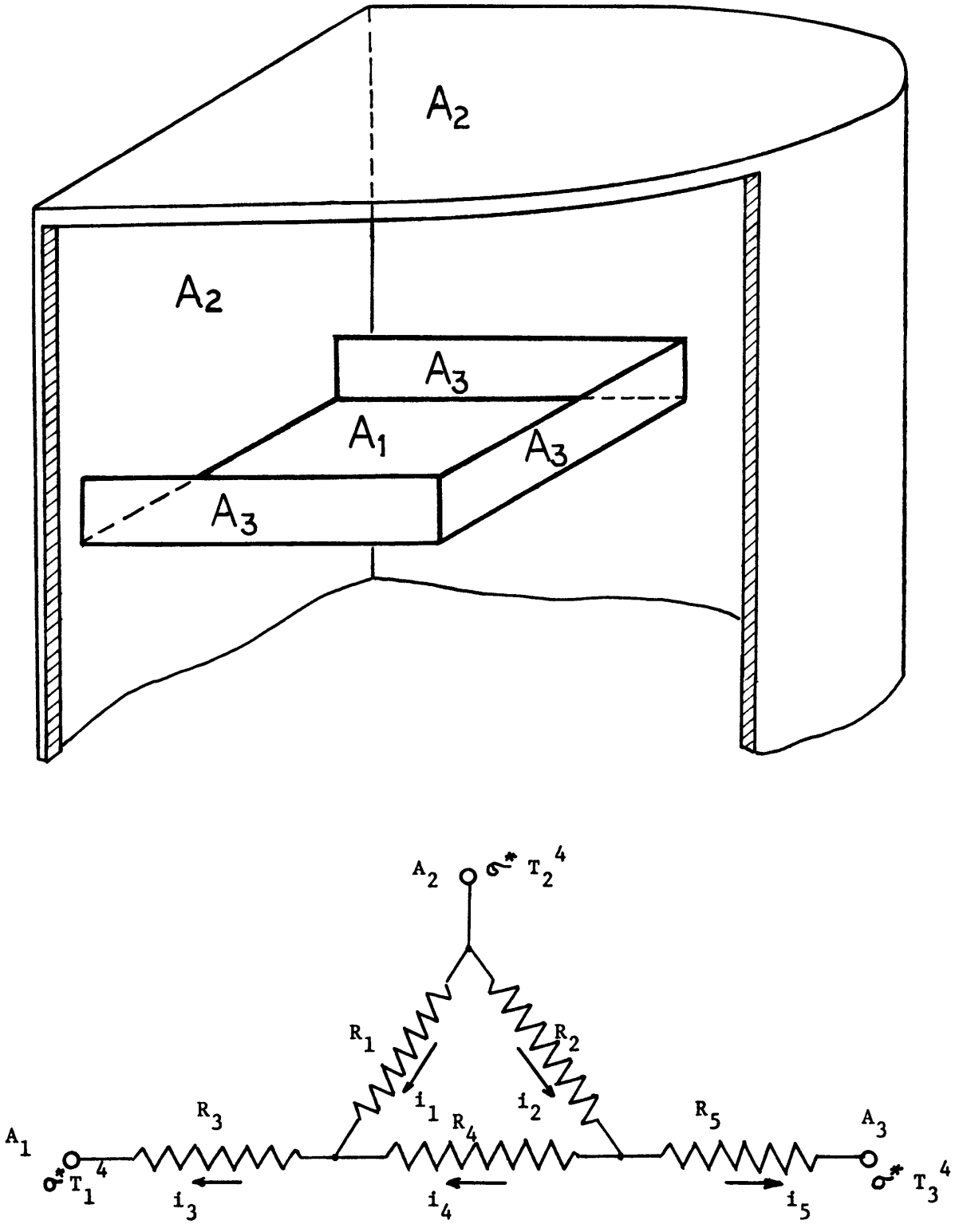

FIGURE 19 RADIATIVE SURFACES AND ELECTRICAL ANALOG

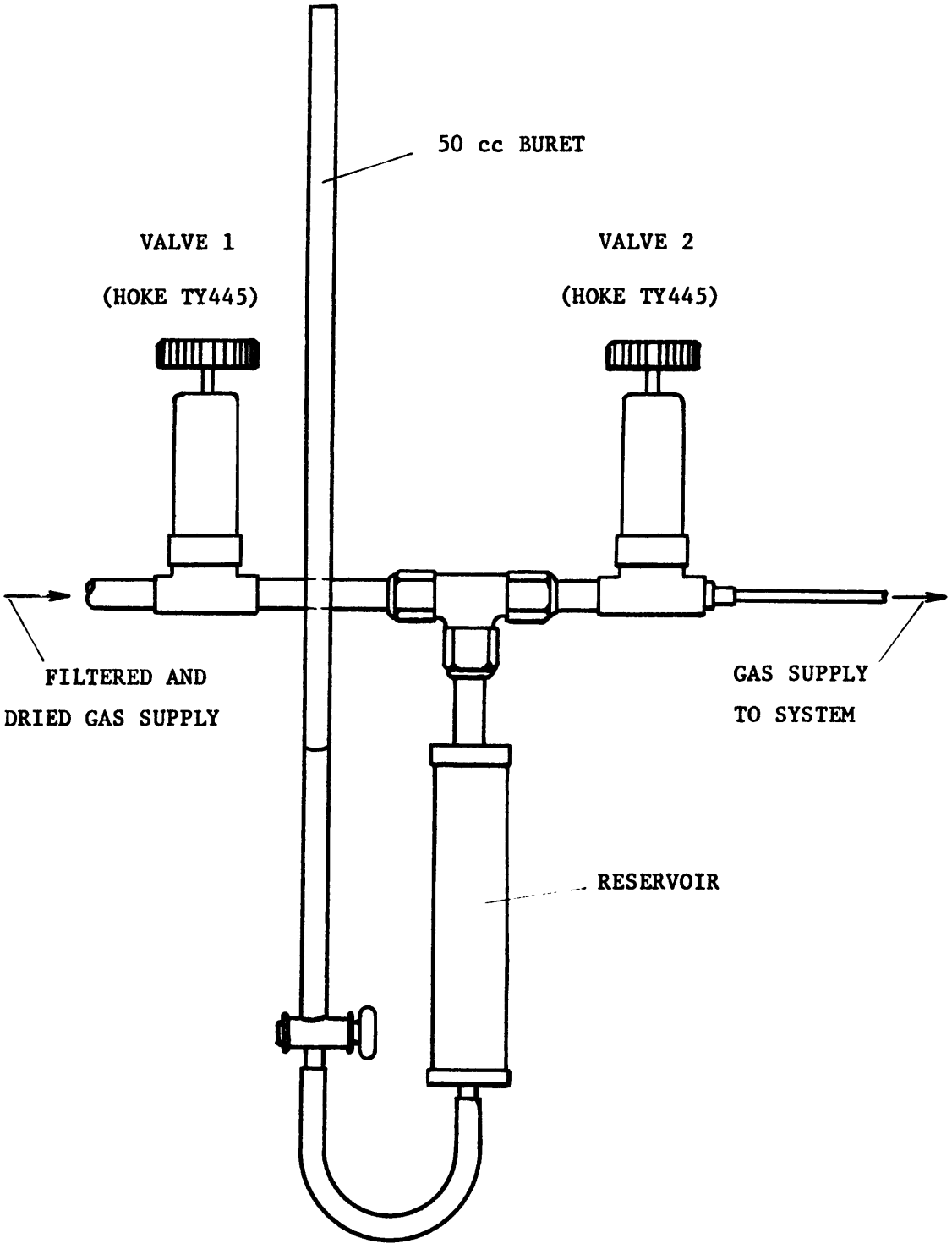

FIGURE 20 INTRODUCTION OF NON-CONDENSABLES

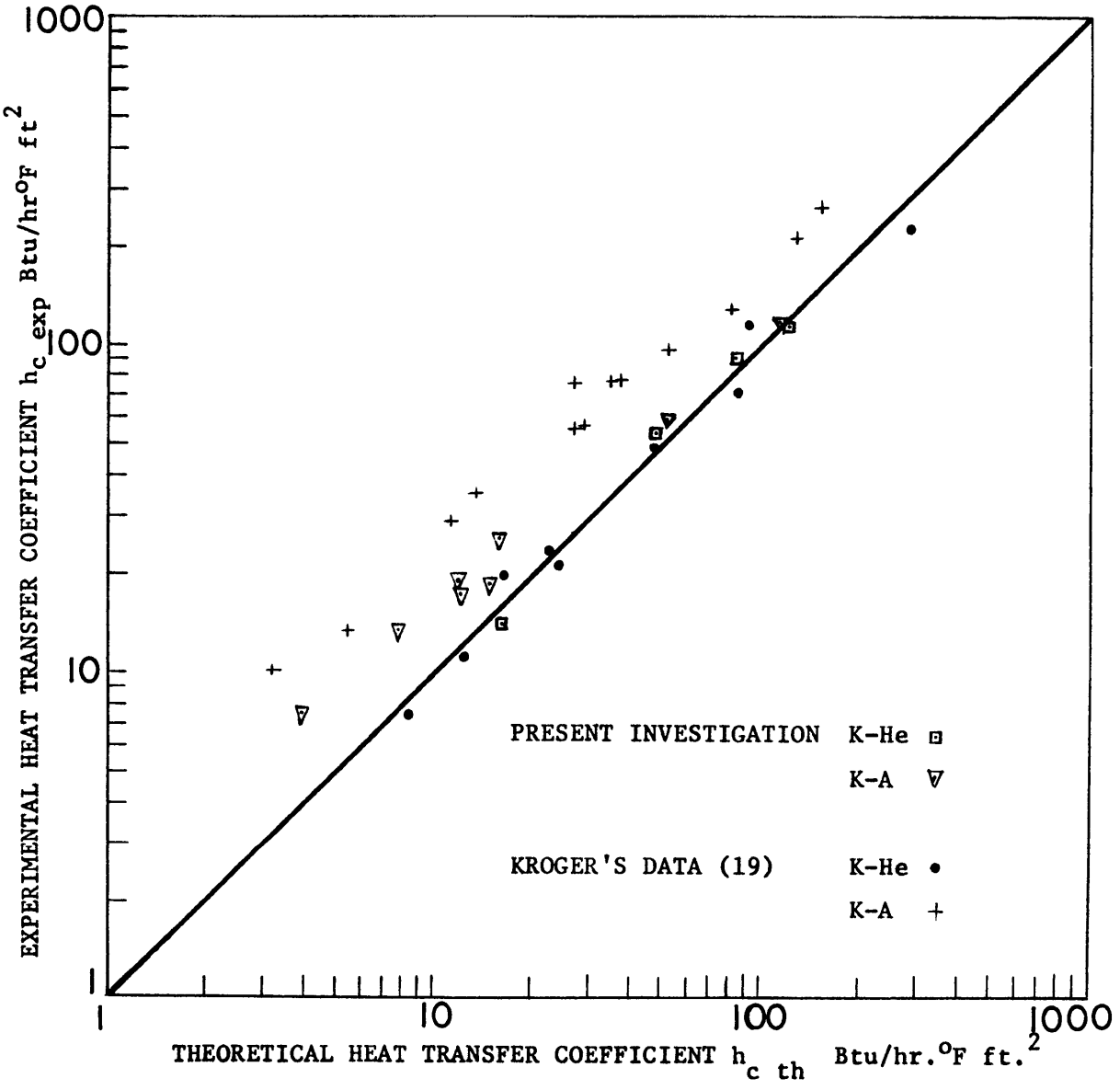

FIGURE 21 COMPARISON OF EXPERIMENTAL HEAT TRANSFER COEFFICIENT TO THEORETICAL HEAT TRANSFER COEFFICIENT

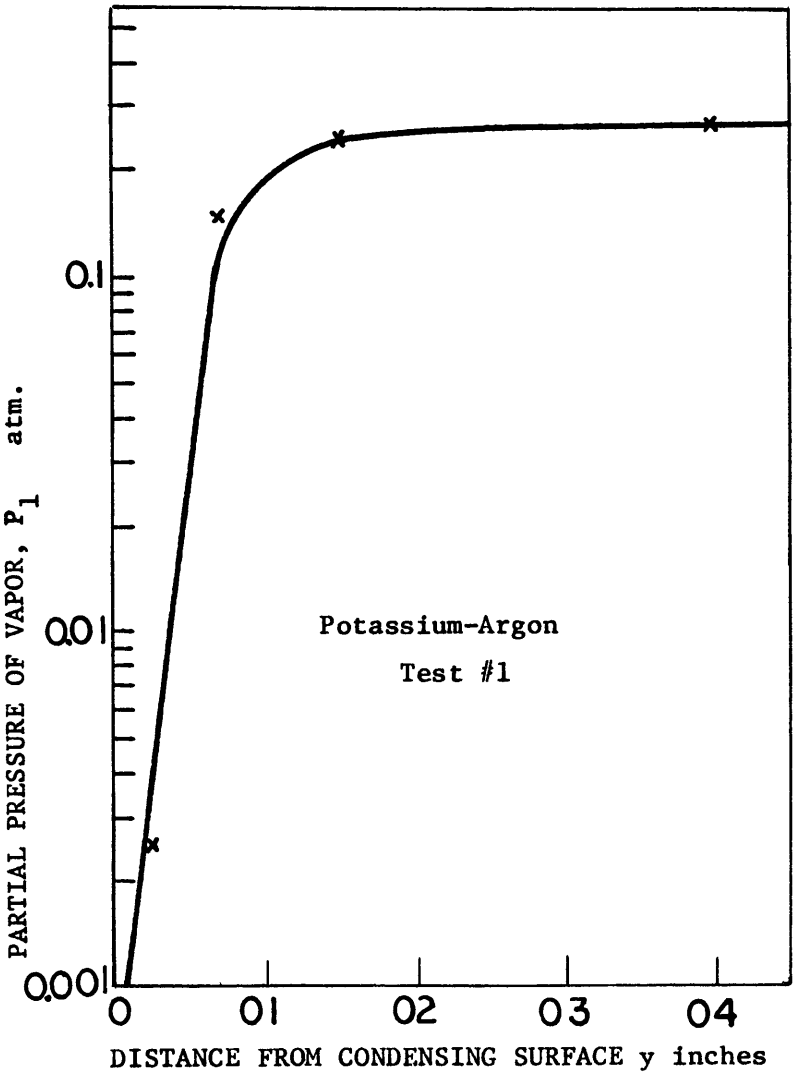

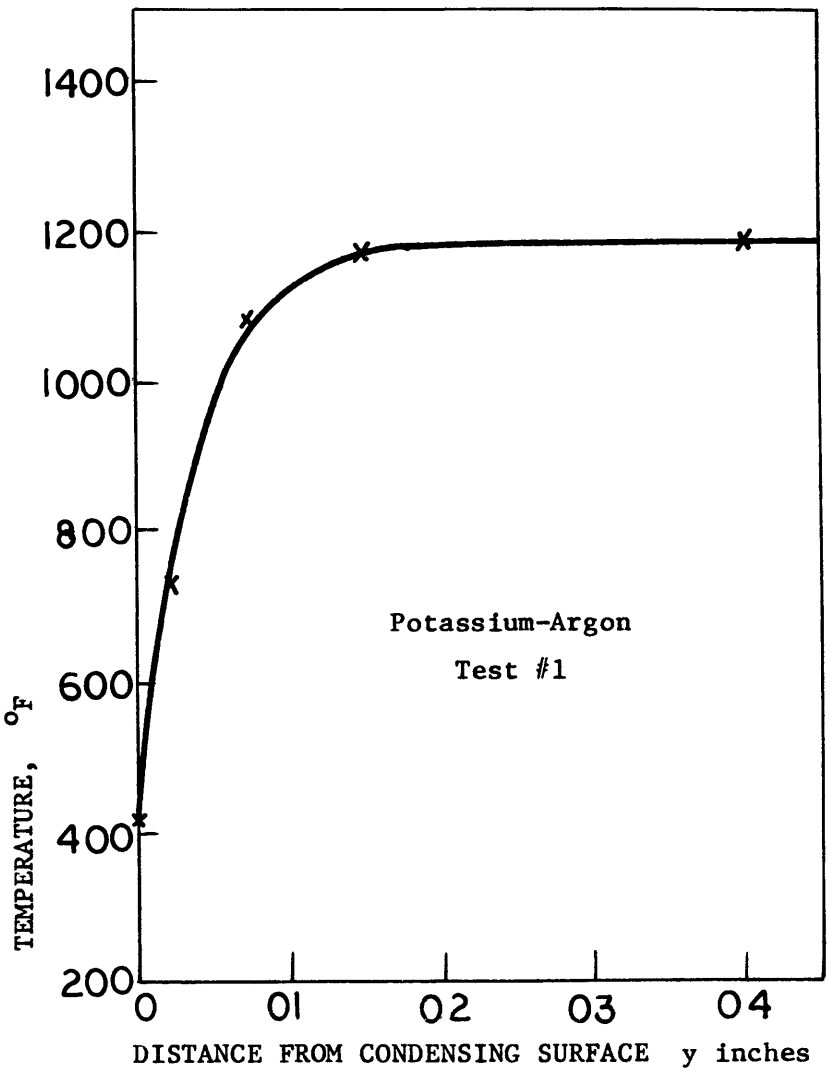

FIGURE 22 PARTIAL PRESSURE AND TEMPERATURE DISTRIBUTION VS. DISTANCE FROM THE CONDENSING SURFACE